THE ROLE OF *ENTEROCOCCUS FAECALIS* BIOFILM FORMATION IN THE REGULATION OF CONJUGATION

A DISSERTATION

SUBMITTED TO THE FACULTY OF THE GRADUATE SCHOOL

OF THE UNIVERSITY OF MINNESOTA

BY

LAURA CAROL CASE COOK

IN PARTIAL FULFILLMENT OF THE REQUIREMENTS

FOR THE DEGREE OF

DOCTOR OF PHILOSOPHY

DR. GARY M. DUNNY

APRIL 2012

Acknowledgements

So many people are responsible for helping me complete my thesis research. First, I want to thank my mentor, Gary Dunny, for his helpful insights and conversations. Throughout the last five years he has kept me excited about my project even when things weren't working out. I hope that someday I can mentor people with the same mix of rational thought and passionate enthusiasm he has. Thank you to all of my committee members for your advice.

All of the members of the Dunny lab helped me in so many ways throughout my thesis research. Thanks to Heather Haemig, Katie Ballering, Thinh Le, Chris Johnson, Kristi Frank, Olivia Chuang-Smith, Frank Barr, Nick Dillon, Yuqing Chen and Anne-Marie Lueck. Thanks Aaron Barnes who spent countless hours showing me what I was doing wrong with the microscope and to Suzanne Grindle for RNAseq processing and analysis. I would like to especially thank Dawn Manias. She has been such an amazing and supportive mentor and always there to listen to my failures or celebrate my successes. I also want to thank all of my wonderful mentees throughout graduate school who have taught me an amazing amount about science and teaching: Francois, Chi, Ben, and Katie.

I appreciate the lessons I have learned from our collaborators Drs. Wei-Shou Hu and Anushree Chatterjee. They taught me more about mathematical modeling than I ever wanted to know but always provided the rationale and explanations to help me understand even the most difficult modeling concepts. I would also like to thank Dr. Jeremy Yarwood for giving me the opportunity to do

an internship in his laboratory at 3M. This was invaluable in my thesis work and a wonderful industry experience.

I would like to thank the members of the Schlievert lab: Tim Tripp, Sara Vetter, Mandy Brosnahan, Kristi Strandberg, Ted Sibley, John Mleziva, Petra Kohler, Evan Henke (E-Train), Jessica Rotschaffer (J-Dawg), Kyle Williams, Alexa Pragman and all of the others who went through the lab. Tim hired me as an undergraduate and Sara mentored me on my first project and without them I might not have ever joined the graduate program. They, along with Kristi and Mandy provided the fun and laughter that kept me going on days when research seemed overwhelming. I would specifically like to thank Pat Schlievert. That fact that he was usually right with all of his crazy ideas gave me the courage to try new things. I greatly appreciate his mentorship both before and during graduate school.

Last but not least, I would like to thank my friends and family. My friends were there to listen to practice talks about things they had never heard of and didn't understand. They were a wonderful way to get away from it all after the science day ended. My family, especially my parents and siblings, are a wonderful source of support and love without which I never would have made it through. Lastly, I want to thank my husband, Gabe, for his patience, love, and understanding. He listened to my problems and helped me make sense of them when he didn't even understand what I was talking about. During the stressful times, he was always there to give me a big hug to keep me going.

Dedication

This dissertation is dedicated to my husband, Gabriel Morton-Cook who kept me sane during graduate school.

Abstract

Enterococcus faecalis has recently emerged as an important nosocomial pathogen. Pathogenicity of these organisms depends greatly on a few important aspect of enterococcal physiology. The ability of enterococci to form biofilms greatly enhances their virulence. Their innate resistance to many antibiotics and their ability to transfer these resistance genes through conjugation heightens their threat to human health. The work described in this thesis attempts to explain the roles of biofilm growth, conjugation, and cell communication in *E. faecalis*. To examine the role of biofilm growth on the *E. faecalis* transcriptome, RNAseq analysis was undertaken. We found that over 100 genes were measurably upregulated during biofilm growth while approximately 26 genes were downregulated. These data gives us important insights into the biology of enterococcal biofilms. In clinical settings, biofilms are likely locations for antibiotic resistance transfer events involving nosocomial pathogens such as *E. faecalis*. Conjugation is an important mode of horizontal gene transfer in bacteria, enhancing the spread of antibiotic resistance. In this work, I demonstrate that growth in biofilms alters the induction of conjugation by a sex pheromone in *E. faecalis*. Mathematical modeling suggested that a higher plasmid copy number in biofilm cells would enhance a switch-like behavior in the pheromone response of donor cells with a delayed, but increased response to the mating signal. Alterations in plasmid copy number and a bimodal response to induction of conjugation in populations of plasmid-containing donor cells were both observed

in biofilms, consistent with the predictions of the model. The pheromone system may have evolved such that donor cells in biofilms are only induced to transfer when they are in extremely close proximity to potential recipients in the biofilm community. These results have important implications for development of chemotherapeutic agents to block resistance transfer and treat biofilm-related clinical infections.

Table of Contents

LIST OF TABLES

LIST OF FIGURES

INTRODUCTION

Enterococcus faecalis, a gram positive bacterium, is a member of the normal flora of the human intestinal tract. Although often non-pathogenic, *E. faecalis* has recently emerged as an important nosocomial pathogen causing infections on indwelling devices such as catheters and heart valves, in the peritoneal cavity and in the urinary tract among others (1, 2). Important characteristics involved in enterococci virulence include intrinsic resistance to antibiotics, the ability to transfer antibiotic resistance genes via conjugation (a form of cell-cell communication), and the ability to form biofilms on many different surfaces. The interplay between these characteristics is of clinical importance and is the focus of my thesis research.

Cell-cell communication in bacteria

The ability of bacterial cells to communicate via secreted molecules is a significant aspect of microbial biology and an important area of research. Inter- and intra-species signaling can coordinate multicellular behaviors such as light production, virulence gene production, biofilm formation, and competence development among others (3-6). Quorum sensing, a type of bacterial communication, involves sensing of bacterial population densities via the use of secreted small molecules. In the case of gram negative bacteria, these small molecules are generally secreted homoserine lactones whereas gram positive bacteria generally employ small peptides.

Recent research has focused on the effects of quorum sensing on altering bacterial transcription patterns and behaviors, but less is known about the role of changing environments on cellular communication. For example, quorum sensing has been shown to enhance biofilm formation in *Pseudomonas aeruginosa* (6), but a larger question that remains is once the biofilm is formed, what are the effects on further cell signaling? For *P. aeruginosa*, growth medium has been found to alter expression of quorum sensing systems greatly (7) demonstrating that although quorum sensing may alter bacterial responses to the environment, the quorum sensing circuits are, in turn, affected by environmental cues.

Bacterial biofilms

Bacterial biofilms are communities of bacteria growing attached to a surface. They are encased in a matrix of their own production that is made up of different combinations of proteins, polysaccharides, and DNA. Many serious bacterial infections have been traced to biofilms including infections on indwelling medical devices and human tissues. In the case of *E. faecalis*, biofilms have been shown to form on heart valves and cause endocarditis. As an important nosocomial pathogen, *E. faecalis* biofilms that form on medical devices are of the utmost importance in human health.

In microbial biofilms, cell-cell communication and coordinated multicellular interactions are of paramount importance. For example, quorum sensing and related forms of intercellular signaling play critical roles in biofilm

development and dispersal (4). Small molecule inhibitors of these signaling interactions show promise as compounds for drug development (8). In addition to communication by extracellular signals, the biofilm environment may contribute to microbial evolution by serving as an important niche for horizontal genetic transfer by transformation or conjugation (9). Moreover, expression of the gene products involved in these processes has been linked to enhanced biofilm formation (5). To determine the extent to which biofilm growth plays a role in transcriptome control, I decided to use a technique known as RNAseq.

RNAseq as a tool for examining the effects of the environment on bacterial gene expression

Recently, RNAseq has emerged as a powerful new technique to examine the transcriptome of bacteria under different conditions. RNAseq is a process that involves high-throughput sequencing to analyze cDNA copied from cellular RNA. The technique allows measurement of total cellular RNA and comparison of transcriptome expression between differing conditions. Transcription profiles of eukaryotic cells including yeast and *Arabidopsis* cells, were published in 2008 (10, 11). As the technique became more popular, articles outlining the transcriptome of eukaryotic organisms became more abundant. In 2010, the first paper was published outlining the use of RNAseq to determine the primary transcriptome of a prokaryotic organism, *Helicobacter pylori* (12). Not only did the authors determine the transcriptome profile *H. pylori*, they also mapped

transcription start sites of these RNAs to determine the extent to which antisense transcription was playing a role in gene expression (12).

As it becomes more accessible, RNAseq will be a powerful tool in the analysis of gene expression profiles of organisms in the near future. Very recently, a paper was published demonstrating the use of this technique to determine gene expression in *P. aeruginosa* biofilms compared to planktonically growing cells (13). With this in mind, I decided to investigate gene expression in biofilm cells and compare it to planktonic cells. Examination of gene expression in *E. faecalis* biofilms has been done on a smaller scale in the last ten years. Data have been collected from promoter activation assays, transposon mutagenesis studies and specific knockout strains to determine gene expression in biofilms but comprehensive genomic analysis on *E. faecalis* biofilms has not been done (14-17).

The role of the biofilm environment on regulation of conjugation

In spite of the plethora of research linking biofilm development to intercellular signaling and genetic transfer, there is limited information about the molecular aspects of cell-cell signaling in biofilms. The inherent heterogeneity of the biofilm environment and extensive gene transcriptome changes may have important effects on both signal production and response. Furthermore, relatively little is known about the molecular interactions between signal molecules and the biofilm matrix and the resulting effects of these interactions on transmission of signals. With regard to gene transfer, transformation in

biofilms has been examined (3) and there is considerable overlap between regulation of competence and biofilm development (18). Numerous studies have described the regulation of conjugation in broth cultures, and it has been shown that the conjugative F pilus promotes biofilm formation (5). Conjugative transfer frequencies have also been measured in biofilms (19), but controlled studies of specific effects of biofilm growth on conjugative gene transfer are limited.

In enterococci, the most efficient conjugation systems are plasmid-borne, and their induction in donor cells is mediated by peptide sex pheromones excreted by plasmid-free recipient cells. Our lab studies the *E. faecalis* pCF10 system, where the signaling molecule is the heptapeptide cCF10 (LVTLVFV)(20). A detailed image describing the induction of conjugation in the pCF10 system is shown in Figure 1.

Since production of cCF10 is encoded within the core genome, the plasmid encodes functions to prevent self-induction of donor cells by endogenous pheromone. These include a membrane protein PrgY which acts to reduce pheromone production by donor cells (21) and the peptide iCF10 (AITLIFI), which acts as a competitive inhibitor of cCF10 (22). Both iCF10 and cCF10 are processed by a protease, Eep, before being exported into the extracellular environment (23). They are both then re-imported into donor cells via the Opp system either alone or in conjunction with the peptide-specific importer PrgZ (24) (Figure 1). The peptides bind to the same site on PrgX, the master regulator controlling initiation of transcription of the conjugal transfer

genes. Although both peptides bind to the same site, they cause different structural changes in PrgX, ultimately stabilizing (iCF10) or destabilizing (cCF10) a tetramer transcription-repressing complex of PrgX and its target sites on pCF10, the primary and secondary binding sites (25) (Figure 1).

The direct effect of pheromone binding to PrgX is to alleviate repression of the *prgQ* operon, which encodes iCF10 and positive regulatory RNAs at its 5'end and the molecular machinery for conjugation in downstream regions, by increasing transcription initiation from the P_Q promoter (Figure 1). Even in the absence of exogenous pheromone, *prgQ* transcription occurs, but it terminates upstream of the conjugation genes, producing a 380 nt RNA called Q_S (26).

Antisense interactions of nascent Q transcripts with a small, complementary RNA called Anti-Q, transcribed from a convergent promoter P_X, shifts the secondary structure of Q to a terminator (27, 28). In uninduced cells there is adequate Anti-Q to block formation of any transcripts longer than Q_S, whereas in the presence of pheromone, the increased production of Q transcripts titrates all of the Anti-Q and leads to longer transcripts (Q_L). Some of these transcripts extend into the genes for conjugation such as *prgB,* whose product promotes donor-recipient aggregation (Figure 1).

Interestingly, the transcription unit encoding PrgX and Anti-Q is convergent with *prgQ*, with 220 bp of overlap. This unique arrangement means that several levels of reciprocal post-transcriptional regulation operate in this system. These mechanisms serve to amplify the primary effect of pheromone,

and recent studies suggested that these multiple layers of regulation confer properties of a bistable genetic switch to the system (29). From the perspective of a donor cell, this peptide signaling system may be viewed as a form of telesensing (30), where donor cells secrete a mixture of the two peptides, with iCF10 present in 50-100 fold excess (22), and monitor their relative concentrations over time. If the ratio changes in favor of cCF10, as is the case when recipients are in close proximity, the conjugation system is activated. It was previously shown that an *in vivo* biofilm, namely an endocarditis vegetation, could serve as niche for high-frequency transfer of pCF10 (31, 32). No previous studies examining the effects of biofilm growth on conjugation have been undertaken in *E. faecalis*.

I became interested in a systematic analysis of peptide signaling and plasmid transfer in biofilms using the pCF10 system as a model. To initiate these studies, I generated a pheromone-inducible fluorescent reporter construct and compared pheromone responses in planktonic versus biofilm cultures. A *gfp* reporter was transcriptionally fused in-frame to *prgB*, the gene encoding Aggregation Substance (Asc10) in the pCF10 conjugative plasmid (Figure 1). As Asc10 production facilitates conjugal transfer of pCF10, the expression of GFP is used as a reporter of conjugation readiness (Figures 1-2). Using this reporter strain, I found a remarkable difference in the population dynamics of the pheromone response under different growth conditions, consistent with the

hypothesis that biofilm growth results in formation of distinct cell types that impact the behavior and regulation of pCF10 transfer.

Following up on these studies and with the help of our mathematical modeling collaborators, I generated a hypothesis regarding the role of plasmid copy number in conjugation. We hypothesized that if the biofilm environment alters the copy number and/or distribution of pCF10 plasmids, this would have a significant impact on induction of conjugation.

In the upcoming chapters, I will describe three separate but related areas of study I undertook during my thesis research. In the first chapter, I will describe the development of a biofilm system in which *E. faecalis* cells are able to grow and form large biofilm communities on glass and polycarbonate surfaces. This system was used to generate biofilm and planktonic cells which were then tested for gene expression using RNAseq. The results of the RNAseq studies are described in the final part of the first chapter.

The second chapter of the thesis describes the induction of the pCF10 conjugation system in *E. faecalis* and the effects of growth in a biofilm on said system. Using an inducible GFP reporter of conjugation readiness, the pattern of conjugation induction is shown to be altered when cells are grown in a biofilm. Using a mathematical model of pCF10 conjugation, we developed a hypothesis that plasmid copy number was altered by growth in a biofilm. The final section of

this chapter describes analysis of plasmid copy number of pCF10 as well as 4 other enterococcal plasmids in biofilm or planktonic populations.

The third and final chapter of the thesis deals with the peptide signals of conjugation and their dual role in directing conjugation and distinguishing between self-/non-self population densities. In the case of cCF10, the peptide can turn on conjugation and allow cells to determine recipient density and, contrarily, iCF10 can both turn off conjugation and signal density of the donor cells. This type of dual role in quorum sensing and conjugation regulation has not previously been identified in other systems.

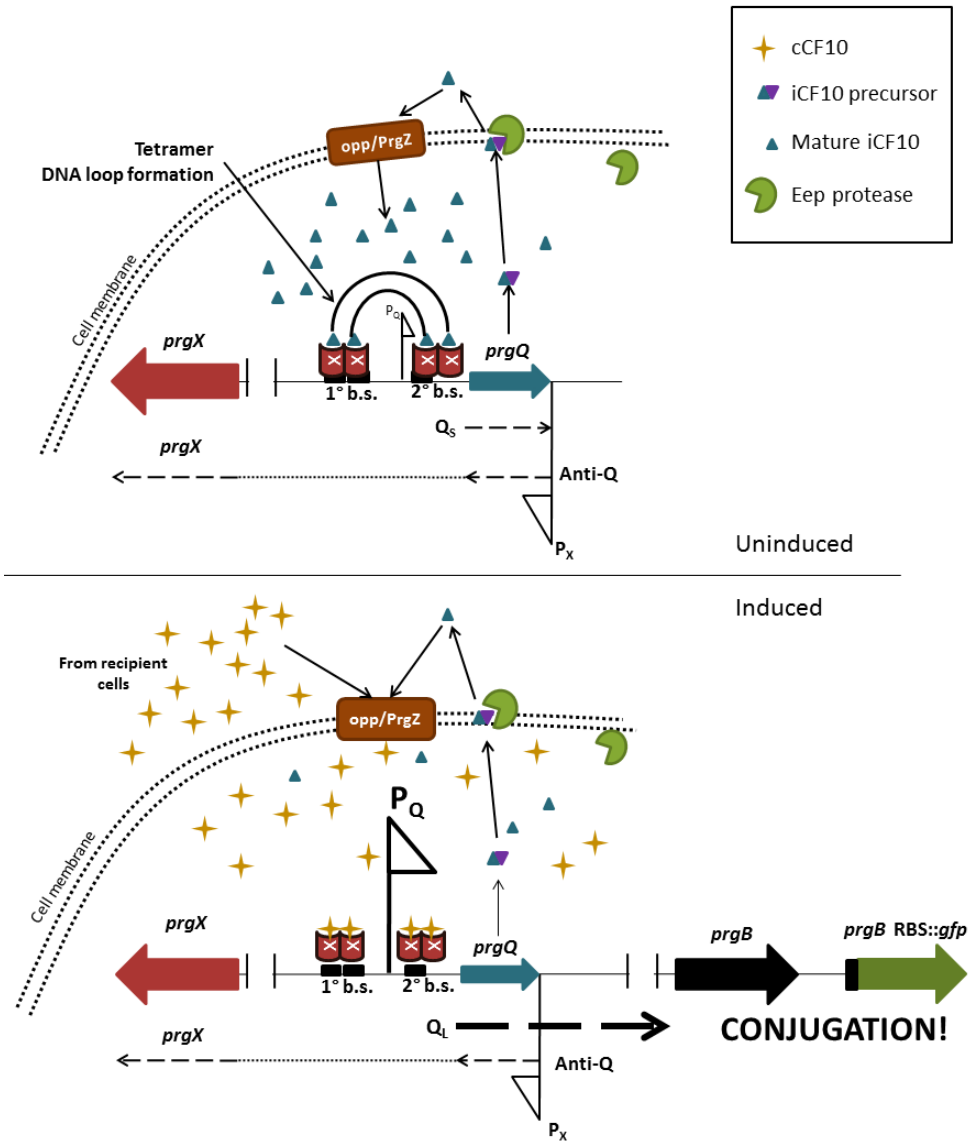

Figure 1: Induction of pCF10. Conjugation in pCF10 is induced by a peptide pheromone produced by recipient cells. As levels of cCF10 in the cell increase, it displaces an inhibitor peptide, iCF10, in the PrgX binding pocket allowing greatly increased transcription from the P_Q promoter and transcription of downstream genes involved in conjugation. The position of the *gfp* gene fusion used in later studies is shown in the bottom panel.

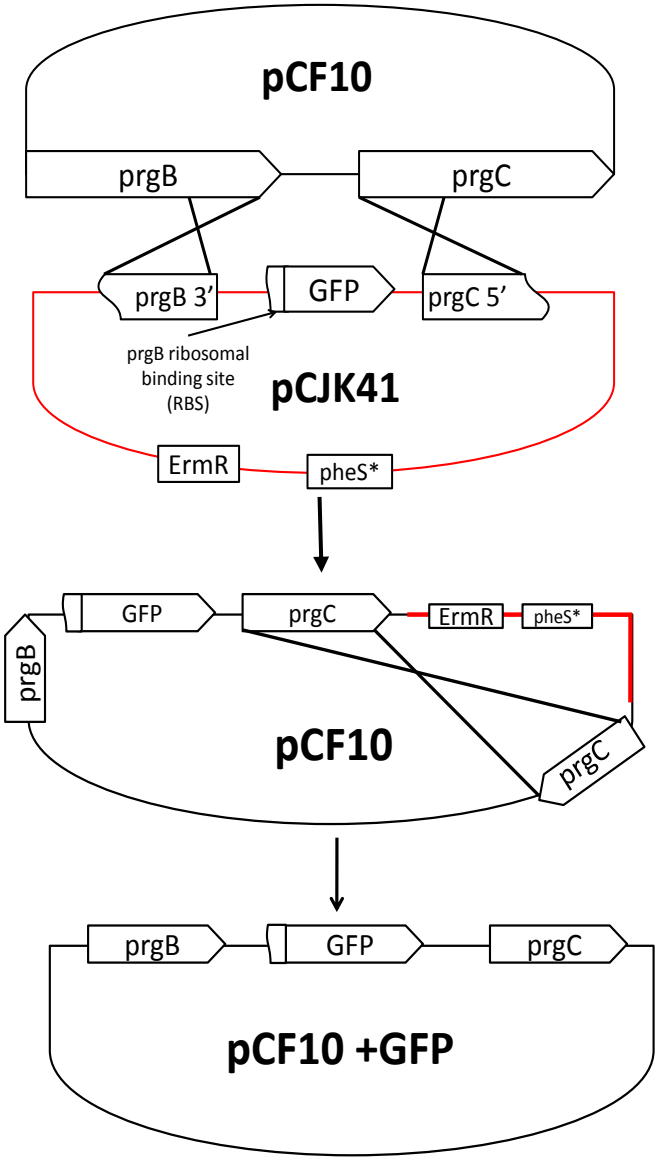

Figure 2: Cloning of *gfp* into pCF10. Using two-step PCR primers (Table 3) and pCJK41 (33), a plasmid was created containing the 3' end of *prgB* and the 5' end of *prgC* flanking a *gfp* gene fused to the PrgB ribosomal binding site. After a double crossover reaction, the pheromone inducible plasmid pCF10-GFP (pCF10-LC1) was created.

MATERIALS AND METHODS

Bacterial strains and media

All bacterial strains are listed in Table 1 and plasmids are listed in Table 2. *Escherichia coli* strains were grown in Luria Bertani medium (Gibco). Todd Hewitt (Gibco) broth (THB) was used to make electrocompetent cells. When required, the following antibiotics were used to supplement the medium in overnight cultures of *E. coli*: 20 μg/mL chloramphenicol (Cl) and 100 μg/mL erythromycin (Erm). MM9YEG medium (referred to as M9) (34), a semi-defined M9-based medium supplemented with 0.3% yeast extract, 1% casamino acids, 20mM glucose, 1mM $MgSO_4$ and 0.1mM $CaCl_2$ was used for all experiments with *E. faecalis* unless otherwise stated. When required, the following antibiotics were used to supplement the medium in overnight cultures of *E. faecalis*: 10μg/mL tetracycline (Tet), 200 μg/mL rifampicin (Rif), 20 μg/mL chloramphenicol (Cl), 50 μg/mL erythromycin (Erm), 1000 μg/mL kanamycin (Kn), spectinomycin (Sp) and streptomycin (St). X-Gal was added at a concentration of 250 μg/mL for blue/white screening in *E. faecalis*. *E. faecalis* strains were grown at 37°C without shaking unless specified.

Table 1. Bacterial strains		
Name	**Relevant Characteristics**	**Source**
Escherichia coli		
EC1000	*E. coli* cloning host, provides RepA in trans; Erm^r	(35)
DH5α	*lac*ZΔM15, *recA1, endA1* mutations for yield and stability	Lab Stock
E. faecalis		
OG1	Reference strain	(36)
OG1S	OG1 St^r	This work
OG1SSp	OG1 Sp^r, St^r	(37)
OG1RF	OG1 spontaneous mutant; Rif^r, Fusidic $acid^r$	(37)
OG1Sp	OG1 spontaneous mutant; Sp^r	(33)
CK111	OG1Sp *upp4::*P_{23}*repA4*	(33)
100-5	OG1Sp contains one copy of *prgX* in the chromosome	(38)
JRC104	OG1RF Δ*ccfA*	(33)
JRC106	OG1RF Δ*eep*10	(33)
OG1S-tdtomato	OG1S contains P_{23}*tdtomato* inserted	This work

Table 2. Cloning vectors and plasmids		
Name	**Relevant Characteristics**	**Source**
pBK1	*prgQ::lacZ* no *lacZ* regulation	(39)
pBK2	*prgXQ:lacZ* pheromone inducible *lacZ* reporter	(39)
pLC1	Cm^r, pBK1 Δ*lacZ*::*gfpmut3b*	(40)
pLC2	Cm^r, pBK2 Δ*lacZ::gfpmut3b*	(40)
pCJK47	Conjugative donor, Erm^r, $oriT_{pCF10}$, P-*pheS**, requires RepA *in trans* for replication	(33)
pCJK47-LC1	pCJK47-5'*prgB::gfpmut3b::*3'*prgC*	(40)
pCJK141	Allelic exchange suicide vector for chromosomal insertions into OG1RF, Conjugative donor, Erm^r, $oriT_{pCF10}$, P-*pheS**, requires RepA *in trans* for replication	C. Kristich, unpublished
pCF10	*E. faecalis* pheromone inducible conjugative plasmid, Tet^r	(41)
pCF10-101	pCF10 Δ*oriT2*	(42)
pCF10-LC1 (pCF10-GFP)	pCF10 *prgB* RBS::*gfpmut3b* inserted between *prgB* and *prgC*	(40)
pMSP3535VAX	*prgX* insertion into pMSP3535VA, Kn^r	(43)
p043lacZ	*prgXQ::lacZ*	(25)
pMSP043	*prgXQ::lacZ*	(44)
pINY8101	pWM402 *prgB::lacZ*	(45)
pJBA110	pUC18Not-$P_{A1/04/03}$-RBSII-*gfp*(LAA)-T_0-T_1	(46)
pJBA111	pUC18Not-$P_{A1/04/03}$-RBSII-*gfp*(LVA)-T_0-T_1	(46)
pJBA112	pUC18Not-$P_{A1/04/03}$-RBSII-*gfp*(AAV)-T_0-T_1	(46)
pJBA113	pUC18Not-$P_{A1/04/03}$-RBSII-*gfp*(ASV)-T_0-T_1	(46)
pBK2-ASV	pLC2 Δ*gfpmut3b::gfp*(ASV)	This work
pBK2-LAA	pLC2 Δ*gfpmut3b::gfp*(LAA)	This work
pBK2-LVA	pLC2 Δ*gfpmut3b::gfp*(LVA)	This work
pBK2-AAV	pLC2 Δ*gfpmut3b::gfp*(AAV)	This work
ptdTomato	Cloning vector containing *tdTomato*	Clontech

Cloning and DNA manipulation

Recombinant plasmids were propagated in *E. coli* DH5α cells prior to transformation into *E. faecalis* unless specified. Transformation was done via electroporation and competent cells were made by diluting overnight cultures 1:10 into 90mL THB and growing for ~2 hours until the OD_{600} was between 0.5-1.0. After 20 minutes of chilling on ice, the cells were pelleted and washed in ice cold 10% glycerol, pelleted again and resuspended in 500 µL of 25 µg/mL lysozyme in 10mM Tris pH 8.0, 20% sucrose, 10mM EDTA and 50mM NaCl. Cells were incubated at 37°C for 20 minutes and then pelleted and washed three times with 1 mL ice cold electroporation buffer (EB) (0.5M sucrose, 10% glycerol). Pellets were resuspended in 200 µL EB, split into 5 aliquots and frozen at -80°C for storage until use.

Plasmid DNA was purified using the Qiagen Spin Miniprep Kit (Qiagen Inc, Valencia, CA). Restriction digests and ligations were done according to accompanying protocols and enzymes were purchased from New England Biolabs (Ipswich, MA). Pfu Ultra II polymerase (Stratagene, Santa Clara, CA) was used for polymerase chain reaction (PCR) DNA amplification on a Techne thermocycler (Bibby Scientific US, Burlington, NJ).

Plasmid and strain construction and induction

pLC1 and pLC2

Plasmids pLC1 and pLC2 were created by PCR amplification of *gfpmut3b* using the *gfp* Forward *Bam*HI and *gfp* Reverse *Eco*RI (primers listed in Table 3)

followed by restriction digest of the *gfp* gene and the pBK1 or pBK2 plasmid. Digestion of the plasmid with these enzymes cut out the *lacZ* gene. The plasmids were then gel purified using the Qiagen Gel Purification Kit (Qiagen Inc, Valencia, CA). The plasmids and *gfp* gene were ligated together to create pLC1 and pLC2 respectively.

pCF10-LC1

To create pCF10-LC1 (Figure 2), the *gfpmut3b* gene was inserted into the pCF10 plasmid using a double crossover method previously described (33). Briefly, approximately 800 base pairs of the downstream region of *prgB*, the ribosomal binding site of *prgB*, the *gfp* gene, and approximately 800 base pairs of the upstream region of *prgC* were joined, in that order, via a two-step PCR method (primers listed in Table 3). This construct was then inserted into the *Not*I site of the multiple cloning region of the pCJK47 plasmid creating pCJK47-LCC1. The plasmid was electroporated into *E. coli* strain EC1000 for propagation and then into *E. faecalis* strain CK111-pCF10-101. This strain was then conjugated with OG1RF recipient cells to ensure delivery of pCJK47-LCC1 into OG1RF cells. Transconjugants were selected based on antibiotic resistance and were then propagated without selection until colonies with the double crossover phenotype were selected for. These colonies were grown overnight, diluted 1:20 in fresh M9 medium and induced using 10 ng/mL cCF10 pheromone. Correct insertion of GFP gave rise to colonies that fluoresced green following a 60 minute induction as measured by a fluorometer using a blue optical kit

(excitation/emission 490/510-570) (Turner Biosystems/Promega, Sunnyvale, CA). The construct was then validated by sequencing.

pBK2-LAA, LVA, AAV, and ASV

To create plasmids pBK2-LAA, LVA, AAV and ASV, the *gfp* Forward *Bam*HI primer and the relevant *gfp* Reverse primer (listed in Table 3 as *gfp* Reverse LAA, LVA, AAV, and ASV respectively) were used to amplify the *gfp* genes from pJBA110, pJBA111, pJBA112 and pJBA113. Following amplification, the tagged *gfp* genes were restriction digested with *Bam*HI and *Eco*RI and ligated into similarly digested pBK2 as above with pLC2. To determine unstable GFP half-lives, overnight cultures grown in M9 + antibiotics were washed and diluted 1:10 into fresh M9 medium. After 60 minutes of growth, 10ng/mL cCF10 was added to the cultures and they were allowed to induce for 60 minutes. Cultures were then washed again and 10ng/mL iCF10 as added to stop induction and shutdown the expression of GFP (downshift). GFP fluorescence was measured using a fluorometer with a blue optical kit (Turner Biosystems/Promega, Sunnyvale, CA) at various times following downshift.

OG1S-tdtomato

pCJK141 was created by Dr. Christopher Kristich to make insertions into the OG1 chromosome between EF1117 and EF1116. P_{23}, a constitutive gram positive promoter, was inserted into pCJK141 at the *Not*I cloning site. Plasmid ptdTomato (Clonetech Laboratories, Mountain View, CA) was propagated in and purified from *E. coli* strain DH5α. Primers were designed with flanking restriction

sites and the *tdtomato* gene was excised from the plasmid and purified using the Qiagen Gel Purification Kit (Qiagen Inc, Valencia, CA). The *tdtomato* gene was fused to the P_{23} promoter in pCJK141 via digestion and ligation. pCJK141- P_{23}-tdtomato was propagated in and purified from EC1000. The plasmid was then electroporated into CK111. A strain of OG1 was selected for streptomycin resistance to create a strain OG1S. OG1S was mated with CK111 to transfer the plasmid into OG1S. After homologous recombination, a double crossover was selected for such that P_{23} fused to *tdtomato* was inserted into the OG1S chromosome. Insertion of the P_{23}-*tdtomato* fusion into the chromosome was verified by sequencing and fluorescence was measured using a fluorometer (Turner Biosystems/Promega, Sunnyvale, CA) with an optical kit with excitation/emission spectra of 525/580-640. Since the excitation/emission spectra of tdtomato are 554/581, this optical kit was chosen for measuring fluorescence (Clonetech Laboratories, Mountain View, CA).

Table 3. Oligonucleotides

Primer name	Primer sequence
gfp Forward BamHI	GGGGATCCATATGCGTAAAGGAGAAGAACTTTTCA
gfp Reverse EcoRI	CGGAATTCTTATTTGTATAGTTCATCCATGCCATGTGTAATC
gfp Reverse LAA	TCTCGAATTCATTAAGCTGCTAAAGCGTAGTTTTCGTCGTTTGC TGCATTGCTTTTGTATAGTTCA
gfp Reverse LVA	TCTCGAATTCATTAAACTGCTGCAGCGTAGTTTTCGTCGTTTGC TGCAGGCCTTTTGTATAGTTCA
gfp Reverse AAV	CTCTCGAATTCATTAAGCTACTAAAGCGTAGTTTTCGTCGTTTG CTGCAGGCCTTTTGTATAGTTCA
tdtomato Forward	TGGGCGGCCGCAGGGAATTCATG
tdtomato Reverse	ATGGATCCTTACTTGTACAGCTCGTCCA

Two-step cloning primers

Primer Name	Primer Sequence
prgB Forward	GTGGCGGCCGCGGACGACATTTCGAAACTAT
prgB Reverse	AATAACTCACGCAACACAAGGCGCTCGTTGCTTTTGTTTGTTGT ACCACATTTCCATTGCACG
prgB RBS Forward	CGTGCAATGGAAATGTGGTACAACAAACAAAAGCAACGAGCG CCTTGTGTTGCGTGAGTTA
prgB RBS Reverse	CTCCAGTGAAAAGTTCTTCTCCTTTACGCATTTGATTCATGTATC ATTCTCCTCGATTTTTTA
*gfp mut3*Forward	TAAAAAATCGAGGAGAATGATACATGAATCAAATGCGT
gfp mut3 Reverse	CTCTTGAATGTTTTCTTCGGTAATTATTTGTATAGTTC
prgC Forward	ATTACACATGGCATGGATGAACTATACAAATAATTACCGAAGA AAACATTCAAGAG
prgC Reverse	GTAGCGGCCGCGTCTATTGGTTTAGTGG

qPCR primers

Gene	Forward Primer	Reverse primer	Amplicon length
prgX	GCTTTGGCTCAATCCTTTG	CTGACTCTCGACCGATTTCTG	198 bp
Q_L	CATGTATATGTTCCCCCGCTTTT	CGGCTCTTACGAGTAGTTCCA	156 bp
gyrB	ACCAACACCGTGCAAGCC	CAAGCCAAAACAGGTCGCC	111 bp

Genomic DNA (gDNA) preparation

DNA preparations were completed using the Qiagen DNeasy Blood and Tissue Kit (Qiagen Inc, Valencia, CA) following the procedure for extraction of gDNA from gram positive cells. Nucleic acid quantification was done using either a Nanodrop (Thermo Scientific, Wilmington, DE) or, for smaller amounts of DNA, the Quant-iT PicoGreen dsDNA kit (Invitrogen, Carlsbad, CA). Using this kit, samples were mixed in black 96 well plates and read on a fluorometer (Turner Biosystems).

If frozen prior to analysis, the samples were immediately pelleted and cell pellets were frozen no more than 16 hours before gDNA preparation. To determine the copy number of pCF10 in planktonic and biofilm populations, gDNA was obtain from 24 hour planktonic cultures, 24 hour biofilms on polycarbonate coupons, sorted cells, and a reference strain, 100-5 containing one copy of *prgX* in the chromosome.

To determine the amount of DNA/colony forming unit (CFU), cultures of OG1RF+pCF10 were grown overnight in M9 medium at 37°C. The overnight culture was then diluted into the CBR and grown as a biofilm (see biofilm growth). The overnight culture was also diluted $1{:}10^5$ into a new conical tube with 15 mL fresh M9 medium. This tube was grown overnight at 37°C. The next day, the coupon biofilms were each vortexed in 15 mL conical tubes with 3 mL PBS + 2mM EDTA to remove adherent cells. 15mL of the overnight cultures and 15mL of the planktonic liquid from the CBR were also collected. Liquid from the

overnight culture (labeled planktonic liquid), the liquid portion of the CBR (planktonic CBR), and vortexed cells from the biofilm (biofilm), were all spun down to pellet the cells. The pellets were then resuspended in the original volume of medium. One milliliter of each culture was removed and diluted to determine total CFUs/mL. Another 1 mL of each culture was diluted 1:10 and 1:100. The DNeasy Tissue kit (Qiagen, Valencia, CA) was then used to extract total gDNA from 1 mL of each culture (undiluted) as well as 1 mL of each dilution for each of the three samples. The extracted gDNA was then quantified used the Quant-iT PicoGreen dsDNA kit (Invitrogen, Carlsbad, CA). Three dilutions of each sample were compared with the plate counts to estimate total gDNA extracted per CFU for three different cell concentrations. These numbers were averaged to attain the final concentration of gDNA extracted per CFU.

RNA extraction and cDNA preparation

Cells were spun down and resuspended in 500 µL PBS + 2mM EDTA and added to 1 mL RNA Protect (Qiagen). After a 5 minute incubation at room temperature, the cells were spun down and either frozen at -80˚C or immediately treated to enzymatic lysis (14). Following lysis, RNA was extracted as described using the Qiagen RNeasy Mini Kit. Two to ten micrograms of total RNA was subjected to Turbo DNase treatment using the rigorous method as described (Ambion). RNA was stored at -80°C. cDNA was prepared using 100-500 ng of total RNA as per the manufacturer protocol using Superscript III first strand

synthesis system kit (Invitrogen) using random hexamers. cDNA was diluted 1:5 in sterile water prior to qPCR.

Quantitative real-time PCR (qRT-PCR)

qRT-PCR was done on gDNA or cDNA using the SYBR green Supermix and an iCycler iQ5 (Bio-Rad) instrument. Each well contained 25µL of total reaction with 200nM primer concentration. Primer efficiencies and C_t measurements were carried out by iQ5 Optical System Software Version 2.0 (2006, Bio-Rad). All experiments met the following criteria for statistical analysis; efficiencies ≥80%, calibration curve r^2 values of ≥0.98, and C_t values for no template control samples ≥35 cycles. Data were analyzed using the Pfaffl method for relative quantification (47). Technical replicates showed no intra-assay variation and were not used in the final statistical analysis.

Biofilm growth and induction

Biofilms were grown using the CDC Biofilm Reactor (CBR) (Bio Surface Technologies Corp., Bozeman, MT). Experiments were done at 37° C except vortexing which was done at 4° C. M9 medium was used as the growth medium for overnight cultures as well as for the batch culture medium. 10% M9 was used in the carboy for the continuous flow portion of growth. The CBR protocol followed the instruction manual guidelines with few minor changes. Briefly, after autoclaving, the reactor and carboy setup were placed in a 37°C room with the reactor on a stir plate rotating at a speed of approximately 125 rpm. Two milliliters of overnight culture at a cell density of approximately $2x10^9$ CFU/mL

were added to the reactor aseptically. The reactor was incubated as a batch culture for 4 hours to allow bacterial attachment to the coupons. At this point, the coupons were either sampled or subjected to a continuous flow of medium at a rate of 8 mL/min for 20 hours, enough to wash out growing planktonic cells. To retrieve the coupons, one polypropylene rod was removed from the reactor, and the three coupons were unscrewed and placed in one well of a 6 well dish. Five milliliters of sterile water were then added to each well, and the plate was placed onto a rotating platform for three minutes to remove planktonic cells.

Coupons were moved to a 24 well plate. Pheromone cCF10 was diluted to various concentrations in 50% M9. One milliliter of the pheromone mixture was added to each well to completely submerge the coupon, and the plate was placed on a rocking platform at 37° C for 0-120 minutes (60 minutes unless otherwise stated). Following induction, coupons were removed to 15 mL conical tubes containing 3 mL of PBS + 2mM EDTA and vortexed for 3 minutes at 4° C to remove attached biofilm cells and break up cell clumps. Preliminary data showed that vortexing for 3 minutes at 4° C gave the highest cell yield and lowest variability compared to sonication and vortexing at room temperature. Quantification of cells was done by making dilutions into PBS + 2mM EDTA and plating dilutions onto BHI plates with appropriate antibiotics and incubating overnight at 37°C.

Serial biofilm growth

Biofilms were grown as above, and all cells were collected after 24 hours. One milliliter of the planktonic cells was used to measure CFU/mL. One coupon was vortexed in 3 mL PBS + 2mM EDTA for 3 minutes. After vortexing, the coupon was removed from the liquid and replaced by a new biofilm coupon. This process was repeated twice to have a total of three coupons worth of cells in 3 mL PBS + 2mM EDTA. Cell counts were done on this liquid and divided by three to determine the approximate CFU/coupon of biofilm cells. The remaining coupons were vortexed as above. All collected biofilm cells were spun down and resuspended in M9 to a final OD_{600} of 0.75. One milliliter of this culture was then added to a new reactor. This process was repeated for 4 days for a total of five days of biofilm growth.

RNASeq

To purify RNA from biofilm and planktonic cells for RNASeq, biofilms were grown in the CBR as described above. After 4 hours of batch growth, the biofilm cells were removed from the coupon surface by vortexing (as above), and 10 mL of the surrounding planktonic fluid were also removed from the reactor and used for planktonic cell RNA. The biofilm and planktonic cells were pelleted and washed once in 1 mL PBS + 2mM EDTA. RNA was extracted and treated with DNase as above. Following DNase treatment, the RNA was treated using the MICROBExpress kit (Ambion, Foster City, CA) as per manufacturer's instructions to purify mRNA and deplete 16S and 23S rRNA. Library creation and RNASeq was

performed by the core facility at the University of Minnesota. RNAseq data analysis was performed by a collaborator (Suzanne Grindle).

RNAseq quality control analysis included trimming of the sequences. This was followed by mapping the sequences to the OG1RF reference genome using bowtie (48). Differential gene expression was determined using the Cufflinks to measure the relative abundance of transcripts in fragments per kilobase of exon per million fragments mapped (FPKM). Cuffdiff was used to take cufflinks expression levels and test them for significant differences. Genes were listed as differentially expressed if the p value ≤ 0.01.

Conjugation experiments

Creation of certain strains required conjugative mating between strains of *E. faecalis*. Matings were done on Brain Heart Infusion (BHI) agar plates (solid mating). Donor and recipient strains were grown to late exponential phase (approximately $2x10^9$ CFU/mL) in BHI and then diluted 1:10 into fresh BHI medium. After 90 minutes of growth at 37°C, the populations were mixed at a donor:recipient ratio of 1:9. Eight hundred microliters of this mixture was spun down and plated onto BHI agar plates without antibiotic selection. Plates were incubated at 37° C for 16 hours. Cells were removed from the plate by addition of 1 mL of PBS + 2mM EDTA followed by scraping. EDTA is used in these and other experiments to break clumps of cells that arise after mating pair formation into single cells. Serial dilutions were plated onto agar medium selective for

donors, recipients, or tranconjugants and incubated for 24 hours at 37°C before counting of colonies.

For measurement of mating transfer efficiencies of biofilm and planktonic cells, overnight cultures of donors and recipients were diluted 1:10 into fresh BHI medium and grown for 90 minutes at 37°C. The cells were then mixed at a donor:recipient ratio of 1:9, and 1 mL of the mixture was added to each well of a 6 well dish. Autoclaved circular aclar membranes (Honeywell Inc., Morristown, NJ) of approximately 1 cm in diameter were added to each well, providing a surface for biofilm formation. The 6 well dish was placed on a shaker at 37°C for 4 hours. Cells remaining in the liquid phase were left in the plate. The aclar membranes were then removed, rinsed twice in sterile water, and place into a new 6 well plate with 1 mL of fresh sterile BHI medium. Both 6 well dishes were then placed back on the shaker at 37°C for 20 hours. Following 24 hours of mating, the liquid cells were collected from the original 6 well dish. Aclar membranes were removed from the remaining plate and rinsed twice in sterile water. The membranes were then place in 2 mL microcentrifuge tubes with 1 mL of PBS + 2mM EDTA and vortexed for 3-5 minutes at 4°C to remove biofilm cells. Biofilm and planktonic cells were then spun down and washed twice in 1 mL PBS + 2mM EDTA. Donors, recipients, and tranconjugants were enumerated as described above.

For measurement of mating efficiencies in donor density experiments, cultures of donor (OG1RF+pCF10) and recipient (OG1SSp) cells were grown

overnight at 37°C in 10mL of M9 medium with antibiotics. Overnight cultures were spun down and washed once in 1mL PBS + 2mM EDTA. The cells were then suspended in 10 mL fresh M9 medium. Donor cells were diluted 1:1, 1:10, or 1:100 in 4.5 mL M9 and 500 µL of recipients were added to each donor dilution. The mating tubes were placed at 37°C. After 30 minutes of incubation, 100 µL was removed from each tube and placed at 4°C. The remaining cultures were placed back at 37°C to continue incubating. One hundred microliter samples were removed at each of the designated time points. After all of the samples were collected, dilutions of the 100 µL samples were plated on donor, recipient, or transconjugant specific agar plates and incubated overnight at 37°C before enumeration. The data shown are averages based on ≥4 biological replicates.

Flow cytometry and fluorescent activated cell sorting (FACS)

Cell suspensions were analyzed via flow cytometry using a FACSCalibur flow cytometer (BD Biosciences, Rockville, MD). Cells were analyzed by size and granularity, and dead cells and debris were gated out of the population. Cells did not require filtering, and the vast majority of cells fell into the same region on the forward and side scatter plot indicating that the majority of cell clumps were broken up by EDTA treatment. Expression of GFP was measured for 100,000-200,000 live cells using the 488 nm laser excitation line. Data from flow cytometry experiments are shown as histograms and contour plots. Data were analyzed using FlowJo (Tree Star, Ashland, OR). FACS was performed using a

FACSAria II and cells were gated, analyzed, and sorted using FACSDiva software (BD Biosciences, Rockville, MD).

Statistical analysis

qPCR data are based on n≥3 biological replicates. In each experiment, ≥2 dilutions were used for each sample to compare to ≥4 dilutions of the control 100-5 DNA. All samples were run in triplicate, and any wells which had standard deviation of ≥0.3 from the other two samples were not used. If removal of one well did not decrease the standard deviation below 0.3, the dilution was not used. Statistical significance was determined by a paired two-sample *t* test (Excel 2010, Microsoft, Redmond, WA). *P* values were considered statistically significant if they were ≤0.01. Exact *P* values are shown in figure legends.

Microscopy

Coupons with GFP-expressing *E. faecalis* cells were counterstained with a red fluorescent Alexa Fluor 594: Wheat Germ Agglutinin conjugate (Invitrogen) labeling the cell envelope and mounted in VECTASHIELD (Vector Laboratories, Burlingame, CA) immediately prior to image acquisition. Images were acquired with a Cascade 1K EMCCD camera (Photometrics, Tucson, AZ) as widefield z-stacks with a 60× 1.4 NA objective (Nikon Instruments, Melville, NY). Z-stacks were taken at 0.2 µm intervals, and were deconvolved using Huygens Pro (Scientific Volume Imaging, The Netherlands). Processed images were aligned and projected as a best-focus composites using MetaMorph (Molecular Devices, Sunnyvale, CA).

Pulse field gel electrophoresis

Pulse field gel electrophoresis (PFGE) was done as previously described with minor alterations (49). Biofilm and planktonic cells from an overnight CBR experiment were grown and harvested as above. Cells were then washed twice and resuspended in 1 mL PBS + 2mM EDTA and chilled on ice. The cells were diluted to final OD_{600} values of 0.86 for biofilm cells and 0.43 for planktonic cells using sterile TE Buffer (10 mM Tris-Cl, pH 8.0, 1 mM EDTA). Plate counts showed that the CFU/mL values at these empirically derived ODs were similar. The gel standard used in this experiment was *Salmonella enterica* serotype Braenderup H9812 (ATCC BAA-664) (provided by the Minnesota Department of Health); *Xho*I was the primary restriction enzyme. The gel was run on a CHEF-DR III System (Bio-Rad, Hercules, CA) at an initial switch time of 2.0 seconds and a final switch time of 10.0 seconds for 13 hours followed by an initial switch time of 20.0 seconds and final switch time of 25.0 seconds for 6 hours. A Gel Doc XR System with Quantity One software (Bio-Rad, Hercules, CA) was used to capture and convert the gel images.

iCF10 donor density and de-induction cell preparation

OG1RF cells containing pCF10 were grown overnight in M9 medium with antibiotics at 37°C. Overnight cultures were spun down and washed once in 1 mL PBS + 2mM EDTA. Cells were resuspended in the original volume of medium and diluted 1:10 into tubes with 4.5 mL M9 medium. The samples were treated as described below prior to RNA extraction.

For donor density experiments, cells were grown for 1 hour at 37°C, and cCF10 was added to the tubes. Four tubes each received no cCF10, 0.1ng/mL, 1ng/mL or 10ng/mL cCF10. The tubes were placed by at 37°C on a shaking platform. After 15 minutes, one tube containing each cCF10 concentration was removed from the incubator, spun down, and washed once in 1mL PBS + 2mM EDTA. This process was repeated at 30, 60, and 120 minutes.

For de-induction experiments, a T=0 sample was taken before 10ng/mL cCF10 was added to the remaining tubes which were then placed at 37°C on a shaking platform for 60 minutes. The five tubes were then removed from the incubator and one tube was labeled as T=60 0i (for 0ng/mL iCF10). These cells were spun down and treated with RNAProtect prior to RNA extraction. The remaining tubes were labeled 120m 0i, 1i, 10i, and 100i. iCF10 was added to the corresponding tubes at 0 ng/mL, 1 ng/mL, 10 ng/mL, or 100 ng/mL. The four remaining tubes were then placed back on the shaking platform at 37°C on a shaking platform for an additional 60 minutes prior to RNA extraction.

Mathematical Modeling

A set of ordinary differential equations based on pCF10 genetic network were developed (Figure 1). Steady state and dynamic simulations were performed in MATLAB (version 2008a MathWorks, Natick, MA). Steady state solutions of non-linear algebraic equations were obtained using MATLAB solve function. ODEs were integrated using function *ode23s* in MATLAB to obtain

dynamic behavior. Mathematical modeling parameters and figure were generated by Drs. Wei-Shou Hu and Anushree Chatterjee.

RESULTS

I. Development of a reproducible system to examine differential gene expression in *E. faecalis* biofilms

E. faecalis biofilms were actively growing and no rapid mutagenic changes selected for biofilm growth

I carried out initial experiments to assess the growth of planktonic and biofilm populations grown in the CDC biofilm reactor (CBR) system. In the 4-8 hour time frame, the population densities of both the biofilm and planktonic cells increased to similar extents and then leveled off (Figure 3). Determination of precise generation times for the two populations in this experiment was difficult because planktonic cells were continually diluted after the initial 4 hours of static incubation, and because both growth and adherence could contribute to the population of biofilm cells. Nonetheless, the parallel increases in both populations suggested that they were both actively growing at similar rates, especially for the first 8-10 hours of the experiments. In this and future experiments, planktonic cells refer to those cells growing in the liquid phase of the CBR system (unless otherwise stated) although similar results were obtained with overnight planktonic cultures.

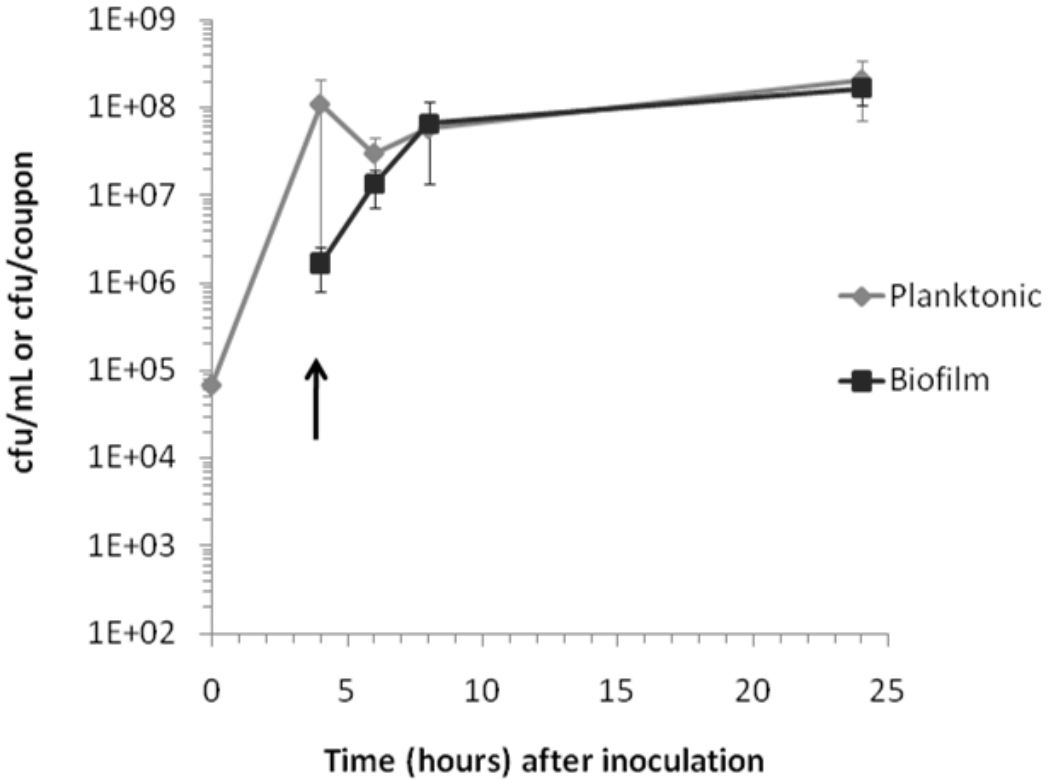

Figure 3: Growth of biofilm and planktonic cells in the CDC Biofilm Reactor.

After 4 hours of batch culture growth, the reactor was operated as a continuous flow system at a rate of 8 mL/min (arrow). The viable populations of biofilm and planktonic bacteria were enumerated by plate counts as described in Materials and Methods. Error bars show standard deviation using n≥3 biological replicates.

To determine whether selection could increase biofilm yield, I performed serial biofilm experiments. In these experiments, cells were grown in a biofilm for 24 hours, removed, washed, and then used to re-inoculate a fresh biofilm. This process was repeated up to 4 additional days. After each day of growth, cells were enumerated on a per coupon basis. Figure 4 shows biofilm and planktonic cell yield from each of the five days. Biofilm cell yield hovered between 10^7 and 10^8 CFU/coupon with no significant increase over the course of five days. This suggests that there was no significant selection for variants with increased biofilm growth during the 24 hour time course of the experiment. Changes in gene expression that occur during early stages of biofilm formation and growth are of great interest, and we used the system described above to obtain early biofilm cells for transcriptional analysis.

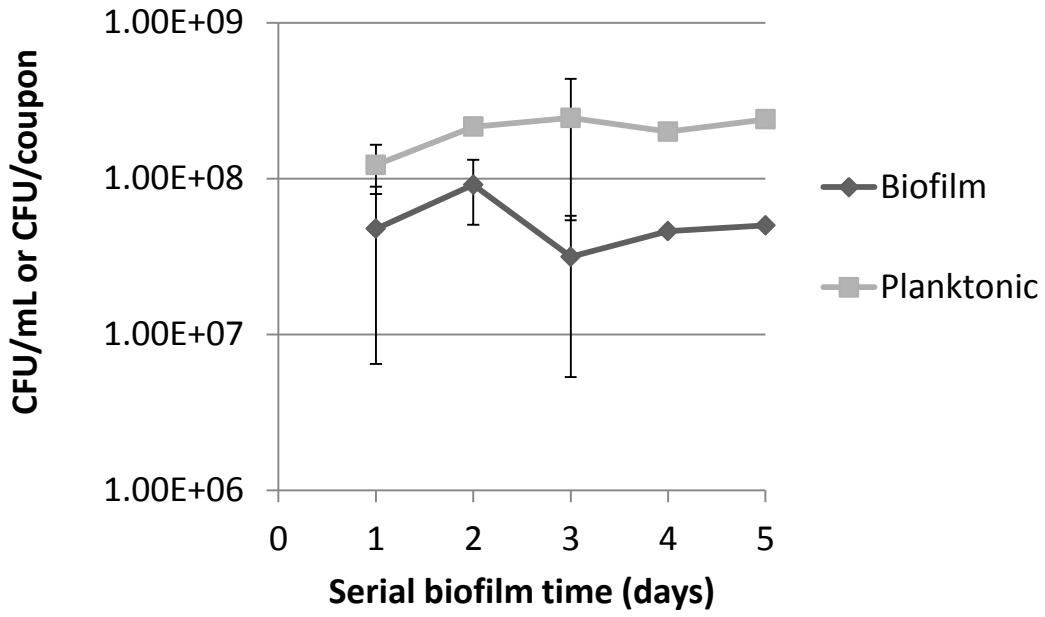

Figure 4. Serial transfer and regrowth of biofilm cells for five days does not significantly increase biofilm cell yield. The light gray line shows planktonic cell counts/mL and the darker line represents average CFU/biofilm coupon. Bars represent standard deviation for n≥3 biological replicates.

Whole transcriptome RNA sequencing showed differential gene expression between biofilm and planktonic cells

RNAseq is emerging as a powerful tool to study the transcriptome of microbial cells under different conditions. We used this technique to analyze the *E. faecalis* transcriptome during the early stages of biofilm growth. We determined the transcriptome using cells growing in a biofilm for 4 hours and compared them to cells growing planktonically in the same CBR. I identified 24 genes down-regulated and 127 genes up-regulated during biofilm growth compared to expression in planktonic growth. Down-regulated genes are listed in Table 4, and up-regulated genes are found in Table 5. The groups of genes that were most often found to be up-regulated in biofilms were ABC transporters, DNA replication and repair enzymes, hypothetical genes, and genes involved in metabolism (Figure 5).

Fifty-one incidences occurred in which genes identified as up-regulated in biofilms according to our RNAseq data had also been previously identified in published and unpublished genetic screens including mutagenesis, transposon studies and promoter trap assays (Table 5). This served as a verification of our data as well as a way to conclude which genes might be strongly associated with biofilm formation. Genes that were very highly up-regulated in RNAseq and also previously found in other studies include those encoding the enterococcal pilus *ebpA-C*, transcriptional repressor *copY*, *recA, oppA,* the quorum sensing system *fsrBC*, and dihydroorotase *pyrC*, among others.

Besides validating previous studies, analysis of the RNAseq data provides insight into the activity of many genes not previously identified to be involved in biofilm regulation. For example, multiple genes in the oligopeptide permease (Opp) system, involved in the transport of peptides, were found to be highly up-regulated in biofilms. As Opp proteins are involved in the transport of both iCF10 and cCF10, the upregulation of Opps could have a significant impact on the pheromone response system (Figure 1). In *Bacillus subtilis*, Opp proteins transport peptides involved in competence development and sporulation (50). The up-regulation of Opp proteins could have important implications in the signaling of cells in biofilms and should be considered and important area of study.

Genes involved in the metabolism and transport of metals such as copper, manganese, and lead were also found to be highly up-regulated in biofilms. It is possible that these genes are up-regulated by cells located in portions of the biofilms that are starved for nutrients. More research is required to determine whether up-regulation of metal metabolism genes is a universal phenomenon or relegated to certain biofilm subpopulations.

Taking a closer look at the metabolism genes, many different pathways were identified to be either up or down-regulated by growth in a biofilm. The pyrimidine metabolism pathway appears to be highly up-regulated with nine genes identified as being differentially expressed (EF1712-1719, EF2396, and EF2738 (Table 5)). Pyrimidine metabolism has been previously identified as being

up-regulated in *Staphylococcus aureus* and *P. aeruginosa* biofilms as well, but the reason for this has not been determined (51, 52). While the EF1712-1719 genes are all up-regulated in response to growth in a biofilm, EF2396 and EF2738 are down-regulated. It is possible that this apparent down-regulation of some RNA transcripts is the result of anti-sense RNA. The presence of anti-sense RNA in the RNAseq data will be addressed in future studies to determine strand specificity of the transcriptome.

Another pathway found to be up-regulated in biofilm growth is involved in pyruvate metabolism. Again this pathway has been previously identified as being up-regulated in *S. aureus* and *P. aeruginosa* biofilms (53, 54). In the case of *E. faecalis,* EF1140 (lactoylglutathione lyase *gloA*), EF1355 (pyruvate dehydrogenase *aceF*), and EF1356 (dihydrolipoamide dehydrogenase *lpdA*) were highly up-regulated in biofilms. These genes are responsible for the metabolism of pyruvate to acetyl-CoA. EF1613, a formate acetyltransferase, *pflB*, was shown to be down-regulated in biofilms. PflB plays a direct role in the conversion of pyruvate to formate. EF1612, the pyruvate formate-lyase activating enzyme *plfA*, responsible for activating *plfB* is also down-regulated in biofilms. This is surprising as the *plfB* homologue was found to be up-regulated in *S. aureus* biofilms and important for glucose consumption and formate production in these cells (53, 55). EF2158, a pyruvate-flavodoxin oxidoreductase was also found to be down-regulated. Further studies will be necessary to characterize whether these genes are truly down-regulated or if these are antisense

transcripts. It is obvious from these data that the metabolism of both pyrimidines and pyruvate play an important role the biofilm environment.

One gene category found to be highly up-regulated in biofilms was that of ABC transporters with over 13 transporters up-regulated in biofilms and two transporters down-regulated. Table 6 lists the types of ABC transporters identified in the RNAseq analysis along with their putative transport substrates. Among these transporters, three had been previously identified in our lab in both *in vitro* and *in vivo* recombinase based in vivo technology (RIVET) screens (14). The identified ABC transporters point to an increased role in nutrient sensing and acquisition in biofilm cells. Because nutrients may be limiting in biofilms, it would make sense for the bacteria to increase their ability to import substrates such as amino acids, metal ions, and sugars (Table 6).

Table 4: RNAseq analysis genes down-regulated in biofilm formation					
EF number	**Description**	**Planktonic**	**Biofilm**	**p value**	**Previously Identified**
EF0104	Arginine deiminase, arcA	99.976	32.607	0.00192905	
EF0108	Arginine/ornithine antiporter ArcD	42.702	13.824	0.00424342	
EF0262	S1 RNA binding domain protein	91.504	278.26	0.00136608	
EF0452	AMP-binding family protein	29.775	8.606	0.00560481	KF RIVET, (14)
EF0633	Tyrosyl-tRNA synthetase , tryS-1	105.62	36.469	0.00298658	
EF0798	hypothetical protein	94.839	28.242	0.00321544	(14, 56)
EF0978	Methenyl-tetrahydrofolate cyclohydrolase, folD	16.273	70.516	0.00113086	
EF1495	V-type ATPase, subunit E	171.41	51.422	0.00141929	
EF1496	V-type ATP synthase subunit C	162.08	51.77	0.00160776	
EF1498	V-type ATP synthase subunit A	146.76	54.211	0.0099222	
EF1510	Protein of unknown function DUF59	155.47	471.35	0.00140751	
EF1533	hypothetical protein	351.71	111.12	0.0017833	
EF1612	Pyruvate formate-lyase activating enzyme, pflA	266.18	81.106	0.00108234	
EF1613	Pyruvate formate-lyase, pflB	490.52	147.4	0.00511915	
EF1752	hypothetical protein	898.72	310.05	0.00337257	
EF2050	ABC transporter, ATP-binding protein	200.88	75.832	0.00634159	(14)
EF2158	Pyruvate-flavodoxin oxidoreductase	31.531	11.282	0.00568888	
EF2396	Uridylate kinase, pyrH	73.088	227.34	0.00121922	
EF2547	hypothetical protein	128.07	837.29	0.00111879	
EF2642	Glycine betaine ABC transport system, OpuAC	85.474	27.989	0.00198982	
EF2738	Alkyl hydroperoxide reductase protein F, thioredoxin reductase	142.45	52.487	0.00898846	
EF3062	Rod shape-determining protein mreC	55.502	170.09	0.00134989	
NEW?	tRNA pseudouridine synthase A	24.257	8.9404	0.00734664	

Table 5: RNAseq analysis genes up-regulated in biofilm growth					
EF Number	**Description**	**Planktonic**	**Biofilm**	**p value**	**Previously identified**
EF0004	DNA recombination and repair protein RecF	54.553	139.75	0.008472 02	KF RIVET
EF0005	DNA gyrase subunit B	65.608	202.4	0.005397 72	KF RIVET
EF0063	Oligopeptide ABC transporter, periplasmic oligopeptide-binding protein oppA	9.7143	60.345	1.15E-05	
EF0066	Holliday junction DNA helicase RuvA	18.243	80.546	0.002674 88	KF RIVET
EF0067	Holliday junction DNA helicase RuvB	39.806	100.13	0.006865 59	KF RIVET
EF0297	transcriptional repressor CopY	0	160.94	7.08E-06	KF RIVET
EF0298	Copper-translocating P-type ATPase	16.391	275.16	3.39E-13	KF RIVET
EF0368	Aspartokinase	18.813	48.096	0.007019 53	KF RIVET
EF0675	L-proline glycine betaine binding ABC transporter protein proX/ Osmotic adaptation	21.06	61.284	0.002135 91	KF RIVET (14)
EF0682	DNA repair exonuclease family protein YhaO	22.982	64.61	0.002948 21	
EF0701	Peptide chain release factor 3, prfC	16.706	49.115	0.002080 7	
EF0704	lipoprotein, putative	8.6872	42.38	0.002835 62	
EF0758	Lead, cadmium, zinc and mercury transporting ATPase	40.674	239.21	6.52E-06	
EF0759	sapB protein, putative	55.175	440.5	2.87E-08	
EF0807	Oligopeptide ABC transporter, oppA	32.715	151.14	2.71E-05	
EF0809	hypothetical protein	200.58	602.62	0.002706 46	
EF0822	hydrolase, haloacid dehalogenase-like family	29.388	79.276	0.009643 8	KF RIVET
EF0858	phage infection protein, pip	28.378	68.776	0.002494 74	
EF0940	Conserved hypothetical protein	39.623	124.01	0.002740 91	KF RIVET
EF1030	endonuclease/exonuclease/phosphatase family protein	15.909	47.763	0.005273 27	
EF1033	6-aminohexanoate-cyclic-dimer hydrolase, putative	10.626	50.122	2.16E-05	
EF1072	galR, galactose operon repressor, LacI family transcriptional regulator	6.5923	45.02	0.004501 27	
EF1084	Universal stress protein family	18.135	136.7	0.002752 66	KF RIVET

EF1085	hypothetical protein	0	235.82	0.000972 89	KF RIVET
EF1091	ebpA endocarditis and biofilm-associated pili A	10.131	104.74	7.51E-10	(14-16)
EF1092	ebpB endocarditis and biofilm-associated pili B	9.17	175.99	2.89E-11	KF RIVET (14-16)
EF1093	ebpC endocarditis and biofilm-associated pili C	15.326	288.1	1.46E-13	KF RIVET (14-16)
EF1097	hypothetical protein	126.68	612.88	1.62E-05	
EF1117	Polar amino acid ABC transporter, permease protein	77.891	337.36	4.88E-05	KF RIVET
EF1118	amino acid ABC transporter, permease protein	53.562	324.01	1.04E-06	
EF1119	amino acid ABC transporter, amino acid-binding protein	68.763	399.15	1.97E-06	
EF1120	amino acid ABC transporter, ATP-binding protein	75.022	363.41	1.49E-05	
EF1133	2,3,4,5-tetrahydropyridine-2,6-dicarboxylate N-acetyltransferase , dapD	68.775	184.84	0.004027 21	
EF1140	Lactoylglutathione lyase, gloA	169.4	423.02	0.007440 91	
EF1141	MutT/nudix family protein	62.541	171.02	0.006235 22	KF RIVET
EF1154	DNA replication protein dnaD	30.332	80.854	0.007641 52	
EF1155	Endonuclease III, nth	36.02	95.971	0.007670 48	
EF1189	Integral membrane protein	21.504	73.349	0.004592 17	
EF1202	Hypothetical protein possible functionally linked with Alanyl-tRNA synthetase	449.08	1205.8	0.005854 93	
EF1203	Putative Holliday junction resolvase	241.21	648.78	0.006886 97	
EF1214	Alpha-acetolactate decarboxylase, budA	19.848	99.152	0.000169 4	
EF1270	COG0779: clustered with transcription termination protein NusA, orthologous to ribosome maturation factor RimP	62.101	236.64	0.000185 88	KF RIVET
EF1355	dihydrolipoamide acetyltransferase, aceF	168.07	522.54	0.008218 73	KF RIVET
EF1356	Dihydrolipoamide dehydrogenase, lpdA	196.45	698.39	0.003110 97	KF RIVET
EF1372	thioesterase family protein, contains CBS domain	28.397	72.651	0.005960 77	
EF1400	cadmium-translocating P-type ATPase	43.514	183.26	0.000273 43	KF RIVET
EF1406	Exonuclease ABC subunit C, uvrC	11.686	31.697	0.005036	

				53	
EF1505	conserved hypothetical protein	31.887	119.78	0.000210 32	
EF1579	SOS-response repressor and protease LexA	125.42	530.49	0.000120 65	
EF1587	MutT/nudix family protein	39.886	137.16	0.000750 17	
EF1596	lipoprotein, putative	28.371	99.394	0.000744 83	
EF1597	Catalase/peroxidase, katA	17.424	65.812	0.000222 48	
EF1599	TPR domain transcriptional regulator, Cro/CI family	60.617	165.29	0.003766 82	
EF1616	Succinyl-CoA synthetase, alpha subunit-related enzymes	97.003	311.25	0.000937 12	
EF1710	transcriptional regulator, LysR family	68.576	199.02	0.003205 73	
EF1711	carbonic anhydrase, putative	42.16	142.45	0.000605 24	
EF1712	Orotate phosphoribosyltransferase, pyrE	55.9	443.93	3.34E-08	
EF1713	Orotidine 5'-phosphate decarboxylase, pyrF	81.975	554.13	3.11E-07	
EF1714	Dihydroorotate dehydrogenase, catalytic subunit, pyrD-2	35.43	237.62	3.46E-07	
EF1715	Dihydroorotate dehydrogenase electron transfer subunit, pyrDII	43.349	278.97	6.49E-07	
EF1716	Carbamoyl-phosphate synthase large chain, carB	65.653	389.38	2.72E-05	
EF1717	Carbamoyl-phosphate synthase small chain, pyrA	80.383	306.42	0.000549 07	
EF1718	Dihydroorotase, pyrC	55.639	232.42	0.000159 03	(14-16)
EF1719	Aspartate carbamoyltransferase, pyrB	91.591	247.06	0.008181 84	
EF1755	Phosphate transport ATP-binding protein pstB	27.122	72.719	0.009121 37	KF RIVET (14-16)
EF1758	Phosphate transport system permease protein pstC	12.556	42.528	0.007842 55	
EF1794	hypothetical protein	33.804	114.14	0.008001 3	
EF1817	Staphylococcal serine proteinase homologue	81.816	386.07	3.76E-05	
EF1818	Coccolysin, gelE	66.45	317.77	9.67E-05	
EF1820	fsrC, histidine kinase	45.055	155.71	1.32E-05	(17)
EF1821	fsrB,	24.339	136.89	1.58E-05	(17)
EF1949	hypothetical protein	49.71	174.16	0.006072 05	
EF1979	ATPase, recombination factor rarA	46.541	141.38	0.002143 77	

EF2072	Cysteine desulfurase, class V aminotransferase	20.99	55.253	0.006183 77	
EF2074	Manganese ABC transporter, ATP-binding protein SitB	165.61	842.06	6.16E-05	
EF2075	Manganese ABC transporter, inner membrane permease protein SitD	154.73	536.62	0.002086 6	
EF2159	Glutamine synthetase type I, glnA	122.07	500.83	0.000737 19	
EF2160	regulatory protein glnR	129.59	438.32	0.000506 6	
EF2203	transcriptional regulator, TetR family	218.88	611.33	0.008166 69	(14)
EF2394	Iron-sulfur cluster assembly ATPase protein SufC	16.762	59.251	0.003507 61	
EF2395	Ribosome recycling factor, frr	111.97	292.09	0.005918 54	
EF2400	RNA methyltransferase, TrmH family	16.702	61.062	0.004394 35	
EF2419	Hypothetical protein	33.818	84.332	0.008195 3	
EF2427	hypothetical protein	19.603	109.08	7.06E-06	
EF2438	PTS system, IIA component	35.837	126.81	0.002202 34	
EF2457	Cell division protein ftsW	21.732	54.345	0.008946 81	KF RIVET
EF2673	GTP pyrophosphokinase	38.866	97.32	0.009908 06	
EF2687	hypothetical protein	20.912	65.561	0.002699 75	
EF2702	hypothetical protein	111.47	377.01	0.000515 17	
EF2704	A/G-specific adenine glycosylase, mutY	13.744	46.43	0.001910 54	
EF2705	Regulatory protein recX	23.579	84.169	0.000825 18	
EF2720	ABC transporter, ATP-binding protein, las	38.157	112.94	0.002497 95	
EF2756	DNA-damage inducible protein P, dinP	18.209	73.576	0.000176 61	KF RIVET
EF2868	conserved hypothetical protein	59.49	142.73	0.009993 61	
EF2870	Hydrolase (HAD superfamily), yqeK	39.103	101.18	0.009845 02	
EF2872	RNA binding protein	0	99.509	0.001641 73	
EF2885	3-oxoacyl-[acyl-carrier-protein] synthase III, fabH	141.35	550.27	0.000838 44	KF RIVET
EF2886	transcriptional regulator, MarR family	338.19	1007.5	0.005544 29	
EF2908	glycosyl transferase, group 2	45.483	135.18	0.001671	

	family protein			66	
EF2909	hypothetical protein	251.74	708.46	0.00284126	KF RIVET
EF2932	Thiol peroxidase, Tpx-type, TSA family protein, AhpC	153.54	420.25	0.00487124	
EF2982	phosphoglycerate mutase family protein, pgm	20.933	87.333	0.00766857	
EF3022	sodium:dicarboxylate symporter family protein	20.967	51.168	0.00915505	KF RIVET
EF3106	Oligopeptide ABC transporter, periplasmic oligopeptide-binding protein oppA	209.15	676.73	0.00706787	
EF3107	peptide ABC transporter, permease protein	131.48	445.17	0.00220562	
EF3127	Guanylate kinase, gmk	44.978	123.97	0.0041405	
EF3131	Hypothetical Protein yicC-like	27.704	81.448	0.0030541	
EF3148	CDP-diacylglycerol--glycerol-3-phosphate 3-phosphatidyltransferase	35.74	120.47	0.00194749	
EF3171	RecA protein	126.07	880.54	2.48E-06	KF RIVET
EF3173	hypothetical protein	17.586	54.265	0.00197108	KF RIVET
EF3177	Hypothetical protein	28.954	91.344	0.0016	(56)
EF3196	Autolysis response regulater LytR	10.332	78.039	0.00272537	
EF3198	lipoprotein, YaeC family	87.178	543.37	1.73E-06	
EF3199	Methionine ABC transporter permease protein	69.845	342.88	1.17E-05	
EF3200	ABC transporter, ATP-binding protein	69.15	330.24	1.63E-05	
EF3209	ABC transporter, ATP-binding protein	9.8698	42.981	0.00601648	
EF3270	Glutathione reductase/metabolism, gor	34.13	90.041	0.00483749	KF RIVET
EF3275	N-methylhydantoinase (ATP-hydrolyzing), hydantoinase/oxoprolinase	0	23.761	0.00011928	
EF3276	Conservative hypothetical protein probably involved in hydantoin, pyrimidine utilization	0	41.344	0.0001965	
EF3283	DNA-binding transcriptional regulator, ctsR	47.978	220.89	7.40E-05	
EF3289	DNA-binding response regulator	133.76	397.55	0.00386889	
NEW?	tRNA pseudouridine synthase A	0	48.037	0.00277283	
OG1RF0016	hypothetical protein	34.998	150.27	5.46E-05	
OG1RF01	DNA-cytosine methyltransferase	127.5	361.99	0.009862	

47	family protein			16	
OG1RF0151	Glycosyl transferase, group 2 family protein	19.336	54.404	0.00884778	
OG1RF0191	D,D-carboxypeptidase, vanYG like	5.9544	258.76	0.00027139	KF RIVET
OG1RF0217	hypothetical protein	29.178	90.416	0.00655996	KF RIVET

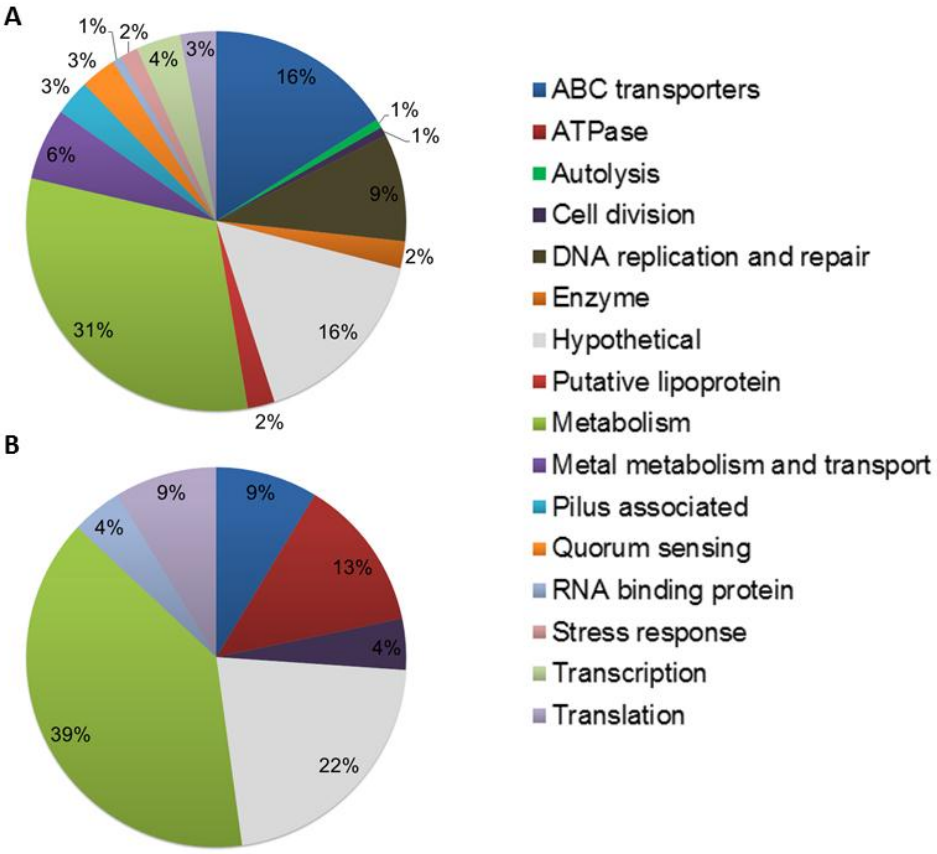

Figure 5. Gene categories found in RNAseq analysis. A pie chart showing categories of genes found in RNAseq to be either upregulated (**A**) or downregulated (**B**) when cells are grown in a biofilm relative to expression in planktonically growing cells.

Table 6: ABC transporters up-regulated in biofilm cells		
EF gene ID	**Putative substrate transported**	**Previously identified**
EF0063	Oligopeptides	
EF0675	Osmoprotectants	(14)
EF0807	Peptides/nickel	
EF1117	Polar amino acids	
EF1118	Glutamine	
EF1119	Glutamine	
EF1120	Polar amino acids	
EF1755	Phosphate	Unpublished RIVET data – Dunny lab, (14)
EF1758	Phosphate	
EF2074	Manganese/iron	
EF2075	Manganese/iron	
EF2394	Iron/sulfur cluster	
EF2438	Glucose/phosphate	
EF2720	Unknown	
EF3022	Glutamate	Unpublished RIVET data – Dunny lab
EF3106	Peptide/nickel	
EF3107	Peptide/nickel	
EF3198	D-methionine	
EF3199	D-methionine	
EF3200	D-methionine	
EF3209	Antibiotics	

Genes involved in homologous recombination were among those highly up-regulated in biofilm formation. EF0004 (*recF*) and EF3171 (*recA*) were up-regulated in biofilms (three and seven fold respectively). Involved in DNA recombination, these genes act during in the process of RecA filament formation. RecF binds to single or double-stranded DNA breaks and requires the action of RecA to complete strand exchange and form a Holliday junction. EF0066 (*ruvA*) and EF0067 (*ruvB*) were also up-regulated in biofilms approximately four and three fold respectively. These genes are involved in the translocation and resolution of Holliday junctions. All four of these genes are considered members of the SOS-controlled response. Deletion of these genes can lead to decreased resistance to stresses such as H_2O_2 as can others identified in this screen such as *katA* (57, 58).

Genes encoding UvrC, required for the removal of UV induced damage, and DinP (damage-inducible protein P), an error-prone DNA polymerase, were also found to be up-regulated in biofilms. A multitude of other putative DNA repair genes were identified in the screen including EF0682 (DNA repair exonuclease *yhaO*), EF1154 (DNA replication protein *dnaD*), EF1155 (Endonuclease III *nth*), EF1203 (a putative Holliday junction resolvase), and EF2705 (regulator protein *recX*). Interestingly, no genes involved in DNA replication or repair were measured to be down-regulated in biofilms. It is apparent that whether or not these cells consider biofilms to be stressful environments, they are highly up-regulating genes involved in their SOS response

and ensuring appropriate mechanisms for DNA replication and repair are present. Another SOS-controlled gene, *lexA*, was also up-regulated in biofilms. Interestingly, LexA acts as a repressor during the SOS response repressing its own expression as well as that of *recA*. Implications of the up-regulation of these genes are expanded on in the discussion section of this work.

Together these data provide us with interesting insights into the transcriptome of cells growing in a biofilm and also act as a complementary approach to the transposon and RIVET studies previously completed in our laboratory (14, 15, 56). The increase in genes involved in metabolism, the SOS response, and environmental sensing will be essential in understanding how bacteria in biofilm communities respond to environmental cues. Further work is underway to determine the strand specificity of the biofilm transcriptome to identify possible biofilm-specific antisense regulators of gene expression.

It is apparent from the RNAseq data that gene expression profiles can vary dramatically when cells are grown in a biofilm. This raises questions as to how regulation of other bacterial functions may be affected by growth conditions. Because of the importance of conjugation systems in *E. faecalis* biology and pathogenesis, I next decided to examine the role of biofilm formation in the regulation of conjugation.

II. Biofilm growth alters regulation of conjugation by a bacterial pheromone

The pattern of conjugation induction differs between cells growing in liquid culture and those grown in a biofilm

Development of an inducibly fluorescent reporter of conjugation allowed us to examine conjugation induction in cells grown both planktonically and in a biofilm to determine the effects of growth conditions on conjugation. Cells containing the pCF10-GFP fusion expressed GFP in response to addition of exogenous cCF10 in liquid culture as well as in biofilms grown in the CBR.

The induction pattern of cells was quantified using either a range of cCF10 concentrations with an induction time of 60 minutes or a set inducer concentration with varying induction times. Flow cytometric analyses of planktonic cell induction patterns are shown in Figures 6A and 7A. As cells were induced with higher concentrations of cCF10, the entire planktonic population shifted to higher levels of GFP expression, apparently homogeneously (i.e. the detection system of the flow cytometer was not able to resolve two distinct populations) (Figure 6A). The histograms are representative of results obtained with pheromone titrations ranging from 0.1-10 ng/mL cCF10. A time dependent unimodal increase in GFP expression was also observed when identical levels of cCF10 were used to induce planktonic cells for time periods ranging from 0-120 minutes (Figure 7A).

When cells growing in the biofilm state were similarly induced, the induction pattern was markedly different (Figures 6B and 7B). At low concentrations of pheromone, a portion of the cells turned on GFP expression and formed a small subpopulation distinct from the larger population. As inducer concentrations increased, the subpopulation expressing GFP increased and the proportion of cells not expressing GFP concurrently decreased (Figure 6B). This suggests that the cells that were non-responsive at low concentrations of pheromone exposure retain the potential to respond to higher pheromone concentrations. If either inducer concentrations or induction times were increased, >95% of cells expressed GFP. A bimodal pattern of pheromone response of biofilm cells was also observed when the time course of the response was examined (Figure 7B). I subjected pheromone-treated biofilms to propidium iodide staining to assess the viability of the GFP –positive and –negative populations, and found very low numbers of potential non-viable cells in either population (<2% in several different experiments, as illustrated in Figure 6D). These data rule out cell death as a reason for the lack of pheromone response in the GFP-negative cells.

The biofilms used for the induction experiments shown in Figure 6 were grown for 24 hours, which produced sufficient numbers of bacterial cells for analysis from a relatively small number of coupons. By substantially increasing the number of coupons, I was able to do similar induction experiments with 4 hour biofilms, and obtained essentially identical results (Figure 8). This suggests

that differentiation of the biofilm cells into distinct sub-populations occurs early in development, while the adherent bacteria are actively growing (Figure 3). Furthermore, I carried out numerous experiments involving induction of planktonic cells (including the planktonic cells from the same reactors used to harvest the biofilms) where the nutrient content of the medium during pre-growth and induction was varied by diluting the M9 growth medium to various concentrations ranging from 10-100%, or by using tryptic soy broth. In all of these experiments a unimodal induction pattern similar to that depicted in Figure 6A was observed, suggesting that biofilm growth was a more important determinant of the bimodal response than nutrient content or growth rate.

The results described above suggest, that at limiting concentrations of pheromone typically produced by recipient cells, the overall frequency of plasmid transfer might be lower in biofilms than in planktonic cultures. I examined this possibility by comparing transfer frequencies in the planktonic and biofilm subpopulations of CDC reactors containing mixed cultures of donors and recipients, and found that the overall efficiency of transfer was significantly lower in the biofilm phase (Table 7).

The biofilm matrix is not responsible for differences between biofilm and planktonic conjugation regulation

A structural component of the biofilm that could cause the biofilm cells to undergo different response patterns from planktonic cells is the biofilm matrix. Most simply, the matrix could inhibit pheromone induction of some cells

by interfering with signal diffusion. The matrix could also serve to concentrate peptides in certain areas to stimulate cell induction in the immediate vicinity. To test for these possibilities, coupons containing biofilm cells were vortexed in PBS + 2mM EDTA to release them from the matrix and suspended in a 50% concentration of M9 prior to pheromone induction. The overall induction pattern of dispersed biofilm cells was the same as that of attached biofilm cells (Figure 6C). This demonstrates that the effects of the biofilm matrix on cCF10 diffusion are not a major factor in the difference responses to pheromone observed between biofilm and planktonic cells. If biofilm cells were resuspended in full strength medium, the population dynamics of pheromone induction reverted to the unimodal mode of normal planktonic cells within 60 minutes.

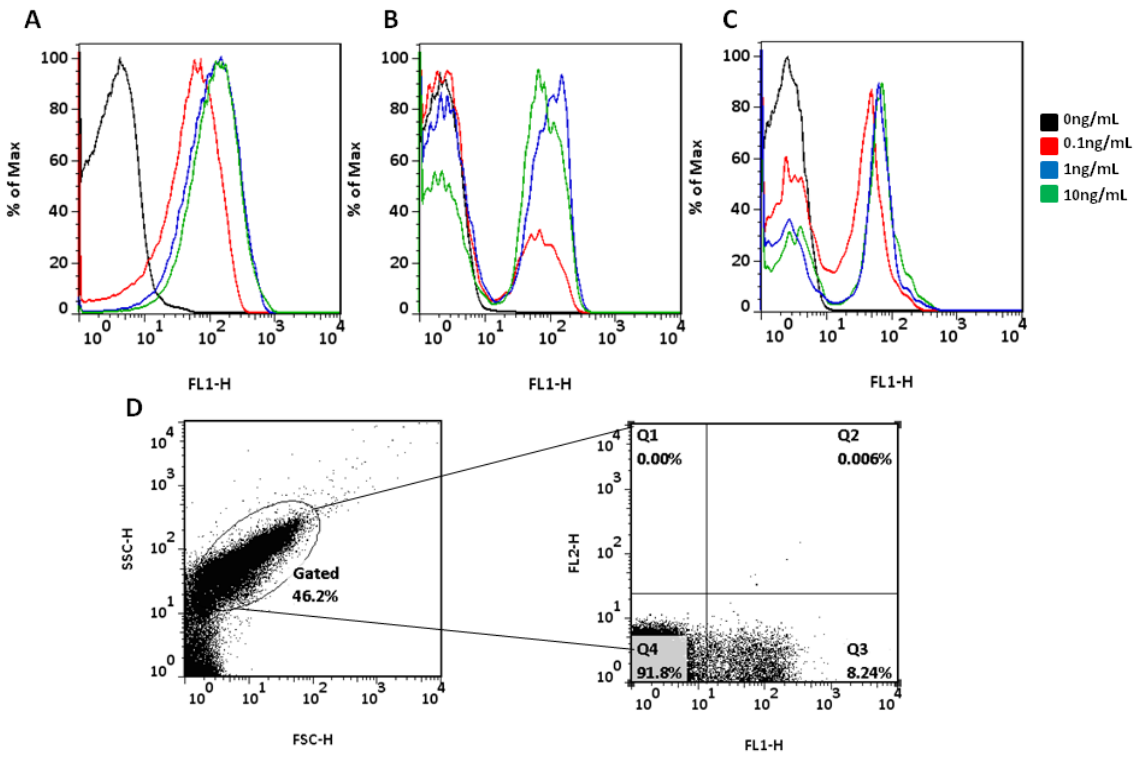

Figure 6. Growth in a biofilm alters the induction pattern of pCF10 conjugation.

A. Cells grown in a liquid culture were induced for 60 minutes with various concentrations of cCF10. Induced populations shifted to higher GFP expression in a unimodal pattern. **B**. Coupons containing biofilm cells were induced for 60 minutes with various concentrations of cCF10. Induced cells expressed GFP in a bimodal population distribution. **C**. Cells grown in a biofilm for 24 hours and then dispersed prior to a 60 minute induction with various concentrations of cCF10 behave as attached biofilm cells showing bimodal response to induction. Horizontal axis = GFP (FL1) expression, Vertical axis = % of maximum cell number. **D.** Flow cytometry analysis of 24 hour biofilms following induction with

1 ng/mL of cCF10 for 60 minutes. Left panel demonstrates the populations gated to remove debris following biofilm dispersal based on size (FSC) and granularity (SSC). Right panel indicating propidium iodide (PI) staining (FL2) on the y-axis and GFP expression (FL1) on the x-axis. Less than 2% of the sorted cells stained with PI; similar numbers were seen with uninduced cells.

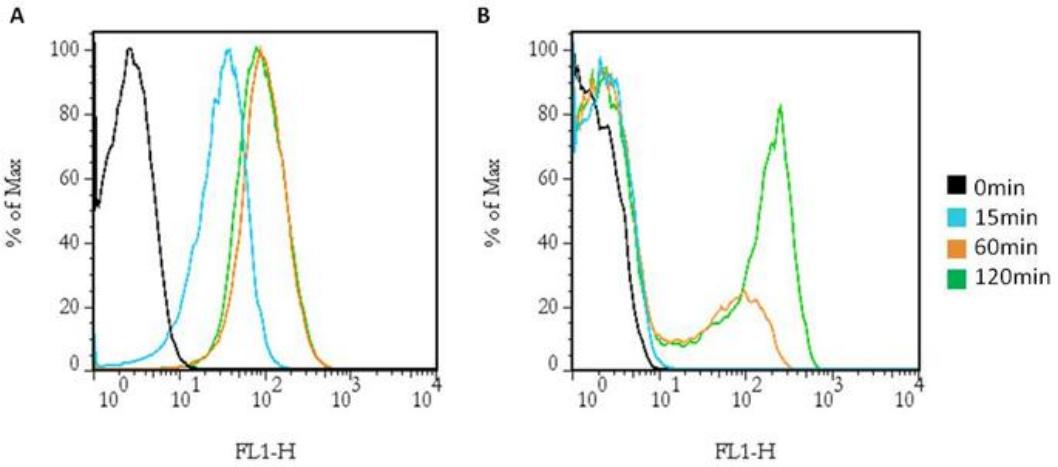

Figure 7. Growth in a biofilm alters the time course induction pattern of pCF10 conjugation. Cells were induced using 0.1 ng/mL of cCF10 and the population distribution of GFP fluorescence was measured over time. **A.** Cells grown in a liquid culture exhibit a unimodal shift pattern in induction. **B.** A time course of biofilm cell induction shows bimodal induction kinetics. Horizontal axis = FL1 (GFP) expression, Vertical axis= % of maximum cell number.

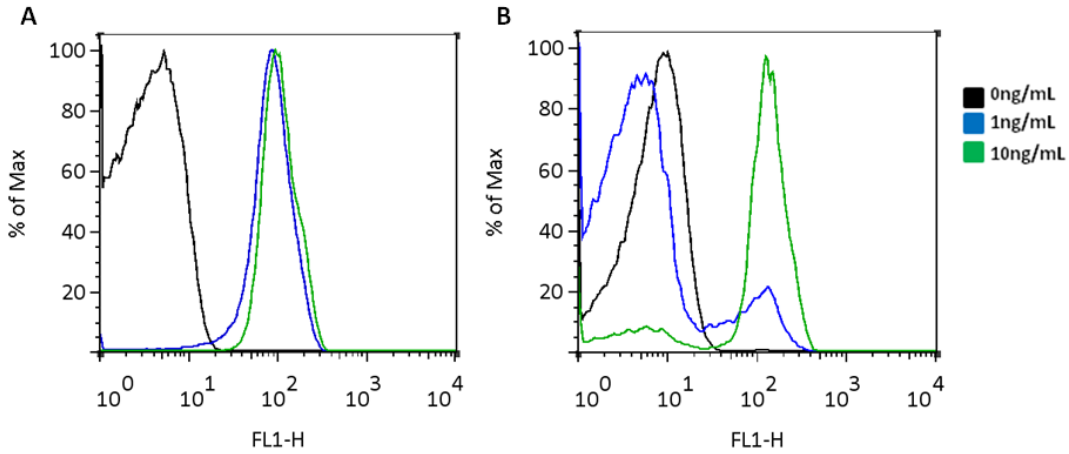

Figure 8. Growth pattern changes are seen as early as 4 hours post biofilm inoculation. A. Cells grown in a liquid culture(**A**) or a biofilm (**B**) for 4 hours were induced for 60 minutes with various concentrations of cCF10. Induced planktonic populations shifted to higher GFP expression in a unimodal pattern. Induced biofilm cells expressed GFP in a bimodal population distribution. Horizontal axis = GFP (FL1) expression, Vertical axis = % of maximum cell number.

We also tested the induction profile of a GFP fusion construct derived from pCF10 where transcription was driven by the same promoter, but the gene encoding pheromone receptor/conjugation repressor protein, PrgX, was deleted. In this case, GFP expression was constitutive, unimodal, and unresponsive to pheromone induction (Figure 9A). Adding *prgX* in trans rescued the bimodal response (Figure 9B). From this I conclude that the bimodal distribution in GFP expression observed with the pheromone-inducible construct arose from biofilm effects on the pheromone response machinery and was not due to random inhibition of GFP expression in a subpopulation of the biofilm cells.

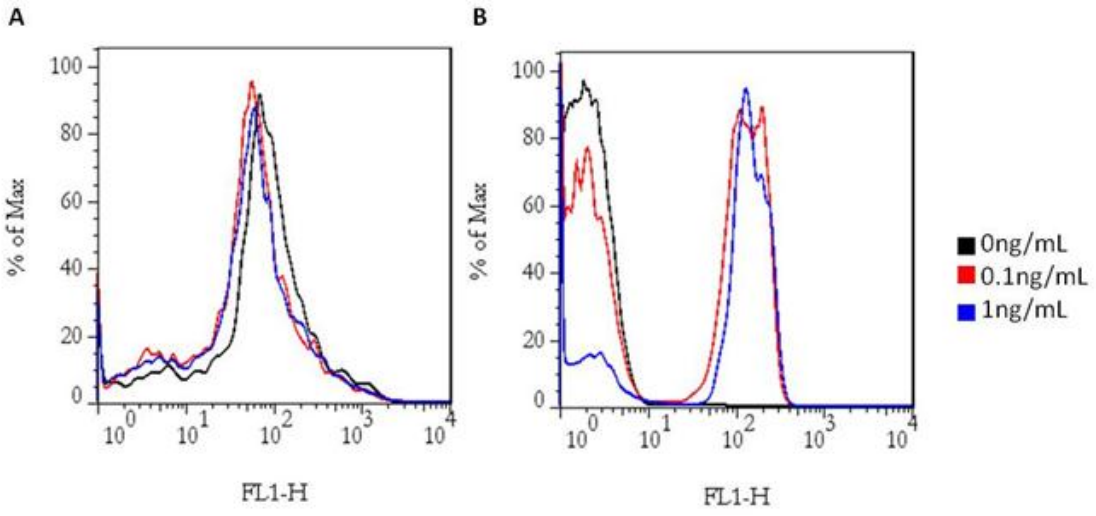

Figure 9. Bimodal induction is not an artifact of GFP expression from the *prgQ* promoter. A. With a constitutively expressed reporter of the promoter P_Q (due to lack of *prgX* repressor gene) virtually all of the biofilm cells are in the "on" state and unresponsive to cCF10. **B.** The same constitutive reporter plasmid demonstrates bimodal induction when the *prgX* is expressed in trans from the chromosome.

Table 7. Biofilm and planktonic mating rates

	Donor CFU/mL	Recipient CFU/mL	Transconjugant CFU/mL	Transconjugant: Donor Ratio
Biofilm	2.46E9	1.28E9	5.6E4	1:43938
Planktonic	1E9	5.9E8	1E7	1:100

RNaseIII and endogenous pheromone production do not promote bistability in planktonic cells

The role of Eep protease and RNaseIII were also examined to see if a deletion in these genes could promote bimodal induction in planktonic cells. Eep is a protease that is responsible for cleavage of pheromone precursors to form mature peptides. Δ*eep* strains do not produce mature iCF10 or cCF10 (23). RNaseIII cleaves double-stranded RNA and can be an important mediator of RNA decay (59). The pCF10-GFP plasmid was mated into strains in which *eep* and RNaseIII had been knocked out. These strains were then tested as above for induction patterns in planktonic cells. Deletion of either *eep* or RNaseIII did not allow bimodal induction in cells grown planktonically (Figure 10A-B).

Using a strain deleted for the chromosomal *ccfA* gene, encoding for cCF10 production (JRC104) I again tested whether endogenous pheromone production alters induction of biofilm and planktonic cells. As above, pCF10-GFP was mated into JRC104 and the cells were examined for induction patterns under biofilm and planktonic growth conditions. Deletion of the gene responsible for cCF10 production did not modify induction patterns in biofilm or planktonic cells (Figure 10C-D). Together, these data suggest that the rate of peptide production and RNA turnover are not the major determinants in the observed differential regulation of conjugation.

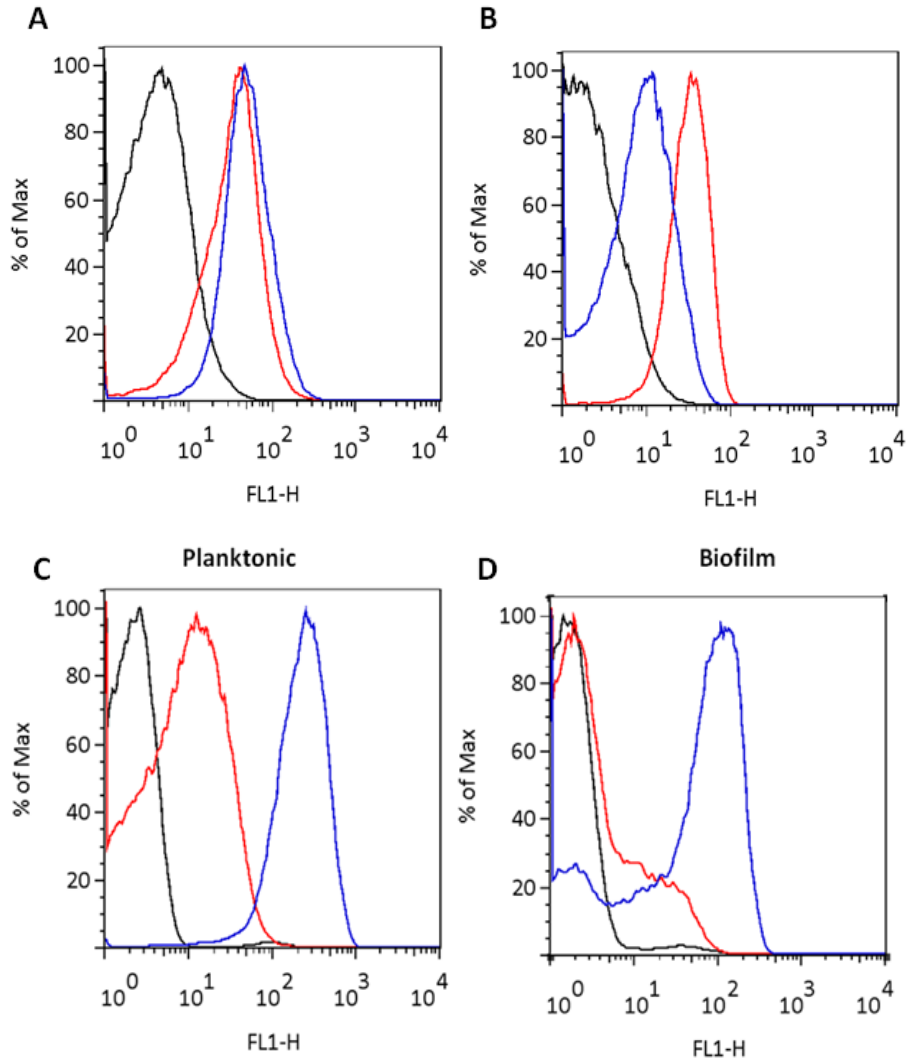

Figure 10. Knockouts of RNaseIII, *eep*, and *ccfA* do not affect the planktonic induction pattern of pLC-2. Planktonic cells deleted for RNaseIII (**A**), *eep* (**B**), or *ccfA* (**C**) or *ΔccfA* biofilm cells (**D**) were induced for 60 minutes with various concentrations of cCF10. Induced planktonic populations shifted to higher GFP expression in a unimodal pattern as seen with wildtype cells whereas *ΔccfA* biofilm cells were induced in a bimodal fashion as seen in wildtype cells.

pCF10 copy number and heterogeneity are increased in biofilm cells

A series of mathematical equations were derived by our collaborators Drs. Wei-Shou Hu and Anushree Chatterjee to model the pCF10 genetic network (40). The details of this model are explained in Cook, et al. 2011, and a summary of the modeling parameters and equations are shown in Appendix IV of this thesis. A characteristic S-shaped bistable response of PrgB to extracellular cCF10 was predicted by Dr. Anushree Chatterjee and is shown in Figure 11. The bistable curve is comprised of three sections: the lower and upper parts of the curve correspond to "off" (low level of PrgB) and "on" conjugation states (high level of PrgB) respectively. The middle section is characterized by multiple steady states, two stable states corresponding to "on" and "off" and an unstable steady state, which is not observed experimentally. This predicted bistable behavior is intrinsic to the gene regulatory network and is predicted to be present both in planktonic cells as well as biofilm cells.

Mathematical modeling further suggested that an increase in the copy number of pCF10 could greatly alter induction responses to cCF10 (Figure 11C). The effect of increased plasmid copy number manifests itself through increased number of binding sites (XBS 1 and 2) available for iCF10 bound PrgX tetramers and cCF10 bound PrgX dimers to bind (Equation S10) and an increase in the number of copies of Q_S and Q_L transcripts per donor cell, which consequently results in increased production of inhibitor iCF10. Donor cells with fewer copies

of pCF10 are predicted to require lower amounts of cCF10 to turn “on” but respond with a lower PrgB expression level than cells with a higher copy number (Figure 11C). Interestingly, increasing plasmid copy number widens the bistable region, suggesting that the “on” and “off” populations are better separated and more easily distinguishable. The model predicts that cells with high plasmid copy number respond slowest to induction and require a higher concentration of cCF10 whereas low copy number cells respond faster and at a lower concentration of cCF10 (Figure 11D-E). A broader plasmid copy number distribution is predicted to give rise to a bimodal population response to low levels of inducer at longer exposure times, such that cells with high plasmid copy number continue to exist in the “off” state even after long exposure time to inducer, whereas cells with lower copy number switch to “on” state (Figure 11D-E). Our model predicts that a higher pCF10 copy number and copy number heterogeneity would enhance a bimodal response to induction with pheromone.

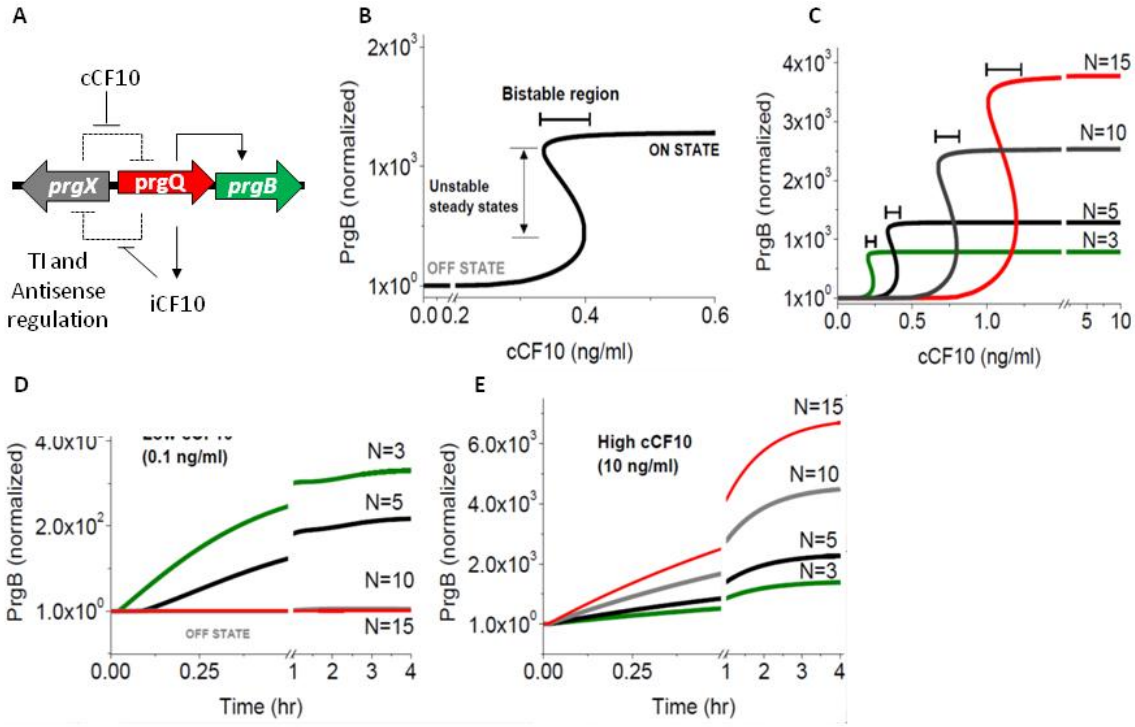

Figure 11. Modeling the effect of pCF10 plasmid copy number (N) on the cCF10 pheromone response. The data illustrated in this figure were produced by simulations based on the mathematical model described in the text and in Appendix IV by Drs. Wei-Shou Hu and Anushree Chatterjee. **A.** A simple schematic of the regulatory circuit of pCF10-based conjugation. The *prgQ* operon encodes the pCF10 conjugation machinery, including an aggregation protein Asc10 encoded by *prgB*. The *prgQ* open reading frame encodes the inhibitor peptide iCF10. The promoters for these operons are located within the same region, but on the opposite strands of pCF10, and produce transcripts that are complementary for 220 nt at the 5' ends. This arrangement leads to reciprocal negative regulation by antisense interactions and transcription interference,

resulting in the double negative feedback loop illustrated by the dashed lines. **B.** Mathematical modeling predicts that the steady state response of PrgB levels to induction with cCF10 shows bistable switch behavior. **C.** Bistable switch response of pCF10 to induction with cCF10 for different plasmid copy numbers. The bistable region increases with plasmid copy number along with an increased threshold cCF10 concentration required to turn "on" the genetic switch. **D-E.** Dynamic response of donor cells with different plasmid copy numbers to low (0.1 ng/mL, (**D**)) and high (10ng/mL, (**E**)) inducer concentrations of cCF10. Cells with high plasmid copy number respond slowest to induction and at a higher concentration of cCF10 whereas low copy number cells respond faster and at a lower concentration of cCF10. PrgB levels shown in **B-E** are normalized to initial state at time t=0 corresponding to "off" steady state levels at 0 ng/mL of cCF10.

The mathematical model predicted that pCF10 copy number changes could alter the pheromone response. Based on this model, I hypothesized that the copy number of pCF10 in biofilms was increased in both average copy number and heterogeneity when compared to planktonic population. To examine this hypothesis experimentally, I performed qPCR on gDNA obtained from pCF10-containing planktonic and biofilm cells to compare the pCF10 copy number of the respective populations. A statistically significant increase in pCF10 copy number of 1.5-2 times that of planktonic cells was observed using qPCR (Figure 12A). A complementary approach using PFGE showed an increase in pCF10 copy number of approximately 1.23 times as determined by band density analysis (Figure 13). The slightly lower estimate from PFGE is understandable based on the band saturation of the pCF10 band in the biofilm cells.

To further examine the relationship between biofilm growth, plasmid copy number and pheromone response, biofilm cells were induced using conditions that generated two approximately equal subpopulations (e.g. Figure 6B). These cells were then sorted based on GFP expression and qPCR was used to examine pCF10 copy number in the “on” and “off” subpopulations. Even though the entire population of biofilm cells was exposed to the same concentration of inducer, the copy number of the pCF10 plasmid differed significantly between cells that expressed GFP and those that did not. Cells not expressing GFP had a statistically higher copy number of pCF10 than cells that expressed GFP during the same induction course (Figure 12B, biofilm). Planktonic cells were also

induced with the same level of cCF10 and cells from the single induced peak were sorted. Cells labeled “on” represent cells from 25% of the peak with the highest GFP expression levels and those labeled “off” are cells representative of the 25% of the peak with the lowest expression of GFP. When cells from these populations were examined for copy number heterogeneity, no statistical difference was observed (Figure 12B, planktonic). This demonstrates that biofilm cells have, on average, higher copy numbers of the conjugative plasmid pCF10 than their planktonic counterparts and also possess a greater heterogeneity in copy number compared to planktonic populations consistent with a mathematical model proposed by our collaborators A. Chatterjee and W.S. Hu. A substantial difference in plasmid copy number was also observed between induced biofilm cells and induced planktonic cells. Planktonic cells contained pCF10 at 3-5 copies per chromosome (Figure 12B, planktonic), while induced biofilm cells possessed plasmid copy numbers as high as 8-15 copies per chromosome (Figure 12B, biofilm).

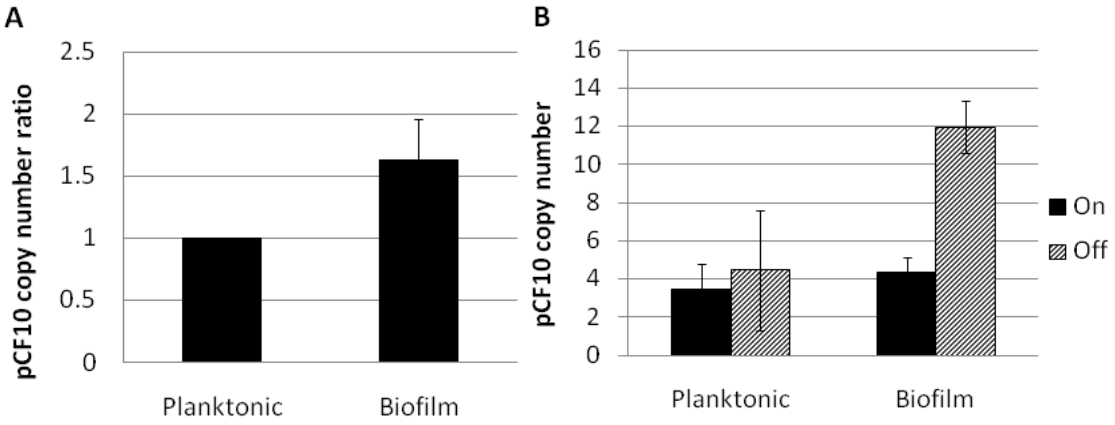

Figure 12. The copy number of pCF10 as well as the population heterogeneity of copy number is increased in biofilm cells compared to planktonic cells. A. Analysis of pCF10 copy number in uninduced biofilm and planktonic cells by qPCR. The average copy number of biofilm cells is 1.81±0.49 times great than that of planktonic cells. n=5 independent experiments. **B.** Comparison of pCF10 copy number in biofilm and planktonic cells exposed to cCF10. Biofilm and planktonic cultures were induced with cCF10 for 60 minutes and sorted into "on" and "off" populations. The sorted subpopulations were then analyzed for pCF10 copy number by qPCR. Induced biofilm cells not expressing GFP had a pCF10 copy number 2.77±0.12 times higher than induced cells expressing GFP. Sorted planktonic populations were not statistically different. All planktonic cells contained 3-5 copies of pCF10/chromosome, whereas biofilm cells contain up to 15 copies of pCF10/chromosome with statistically significant heterogeneity between the "on" versus "off" subpopulations. n=4 independent experiments ±

and error bars represent standard deviation ** P value <0.02 ***P value < 0.003

P values were calculated using a two-tailed t-test assuming equal variance.

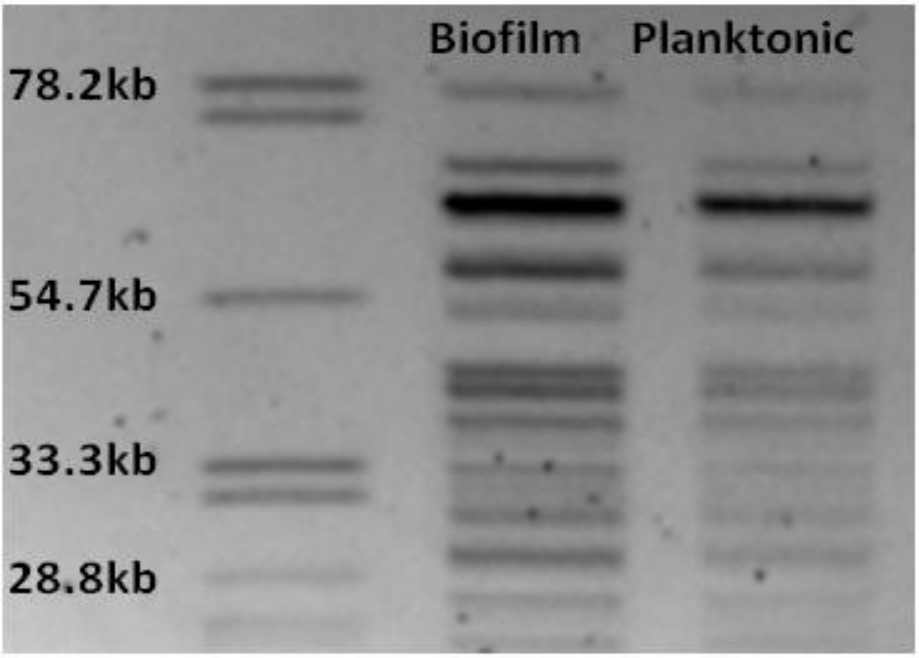

Figure 13. Pulsed field gel electrophoresis (PFGE) to examine cell copy number. PFGE of biofilm and planktonic cells shows that biofilm cells have a higher pCF10 DNA/chromosomal DNA ratio than planktonic cells. Arrow indicates pCF10 band. Using three different chromosomal bands for reference, the ratio of biofilm pCF10/planktonic pCF10 = 1.23±0.01

The copy number of various enterococcal plasmids is altered by growth in a biofilm

We hypothesized that the increased plasmid copy number phenomenon we observed in biofilm cells was not restricted to pCF10. To examine this hypothesis, we chose four plasmids with four different replicons representing both methods of plasmid replication (rolling circle and theta replication) (Table 8). These plasmids all contain the *prgX* gene, which we used to compare the number of copies of the plasmid to the 100-5 strain which contains one copy of *prgX* on the chromosome. The biofilm and planktonic growth and copy number analysis were done as previously described for pCF10.

We found that all four plasmids were statistically increased in copy number in biofilm cells when compared to their planktonic counterparts. The plasmid copy number in biofilm cells was between 1.6-2xs higher than the copy numbers in planktonic cells (Figure 14A). This phenomenon was present regardless of the native plasmid copy number of the four replicons (Figure 14B).

One explanation for differing copy number measurements is that the amount of gDNA could be higher in planktonic cells. This would cause the ratio of *prgX* to *gyrB* to be skewed and thus make it appear that biofilm cells had more copies of the plasmid when in fact they only had fewer copies of the *gyrB* gene. To test for this possibility, total gDNA/CFU was measured. We found that the total amount of gDNA/CFU was the same between biofilm and planktonic cells

whether the planktonic cells were harvested from the reactor or from an overnight culture (Figure 15).

Although gDNA content does not appear to play a role in the copy number phenomenon, I examined early biofilms to ensure that growth rate was not affecting our measurements. One plasmid, pMSP3535VAX was chosen and grown in the CBR for 4 hours. Planktonic cells were removed from the liquid portion of the reactor and biofilm cells were collected from the coupons. Copy number analysis was done to determine whether young biofilms, which should retain high growth rates (Figure 3), still have differential copy number expression. Results from four biological replicates show that the copy number of biofilm cells is higher than planktonic cells even as early as 4 hours post-inoculation of the biofilms (Figure 16).

Table 8. Enterococcal plasmids for copy number measure

Plasmid	Replicon	Replication	Source	Antibiotic resistance
pBK2	pCI305/pBR322	Rolling circle	(60)	Chloramphenicol
pMSP3535VAX	pVA380-1	Rolling circle	(43)	Kanamycin
p043lacZ	pAT18/pAMβ1	Theta	(61)	Erythromycin
pINY8101	pWM402/pIP501	Theta	(45)	Chloramphenicol

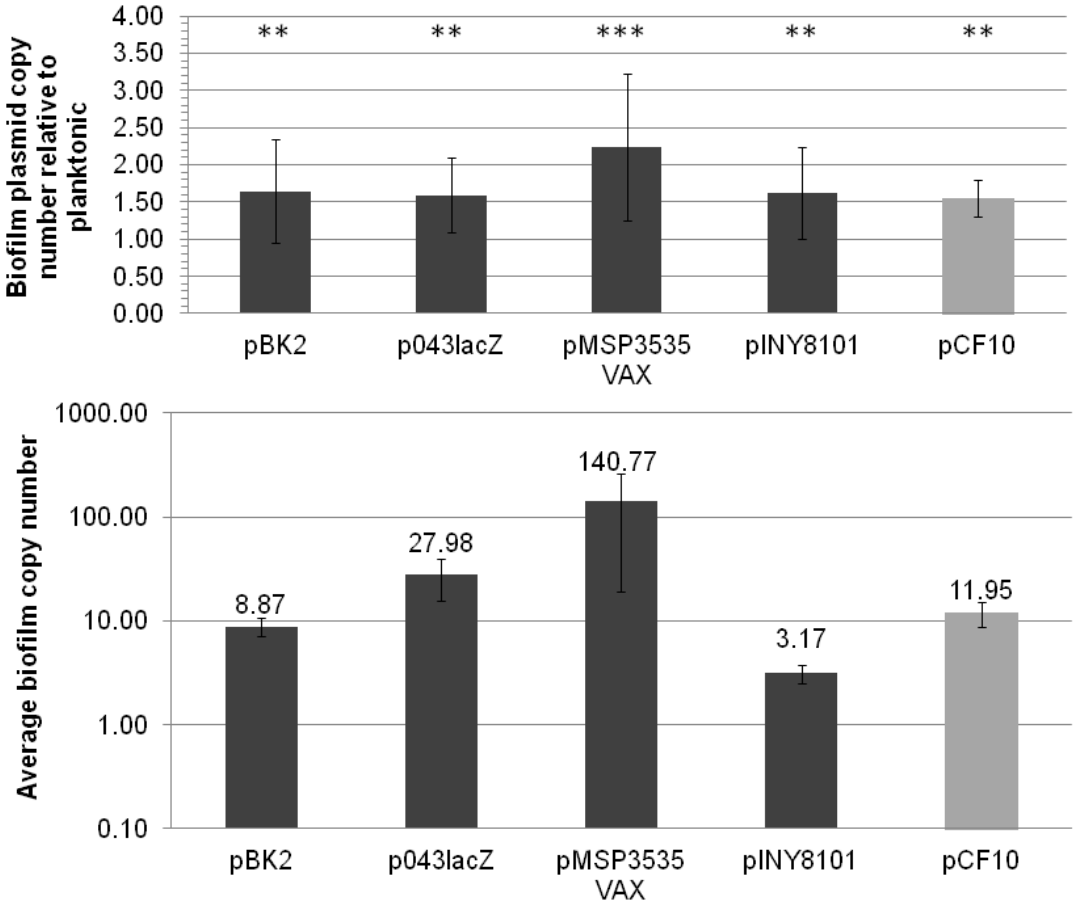

Figure 14. The copy number of four different plasmids is increased during biofilm growth versus growth in liquid culture. A. Plasmid copy number is shown as a ratio to planktonic copies. Copy numbers are measured per chromosome. **B.** The average copy numbers of the four plasmids range widely from ~1-150 copies/chromosome. **=p value ≤ 0.05 ***=p value ≤ 0.001 (original pCF10 data reported in (40) and shown in Figure 12A).

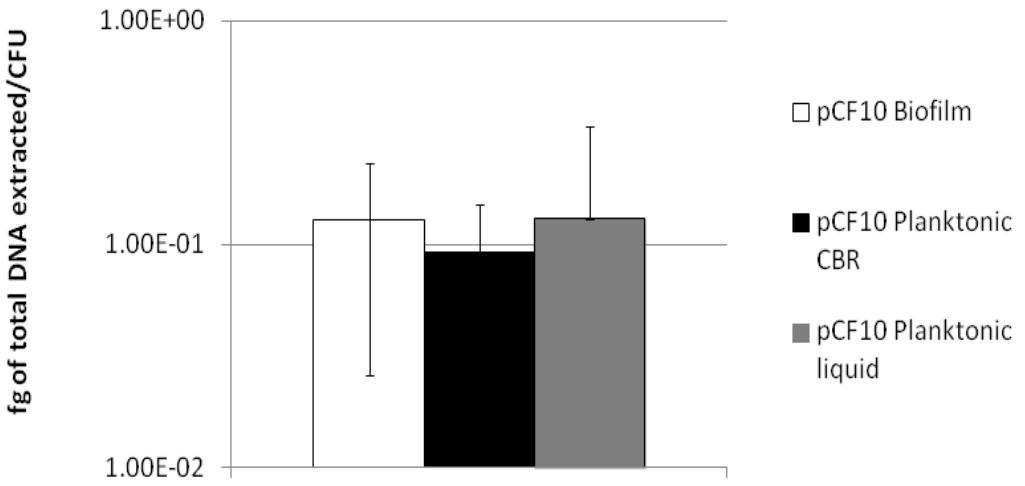

Figure 15. The amount of total gDNA/CFU extracted is the same for biofilm and planktonic cells. Approximately 0.05-0.5 fg of total DNA was extracted per CFU from cells grown in a biofilm, in the liquid phase of the biofilm reactor, or in a liquid overnight culture. No statistical difference was seen between total DNA extracted from the three populations indicating that the number of chromosomes per cell is not significantly altered in these three environments after 24 hours of growth.

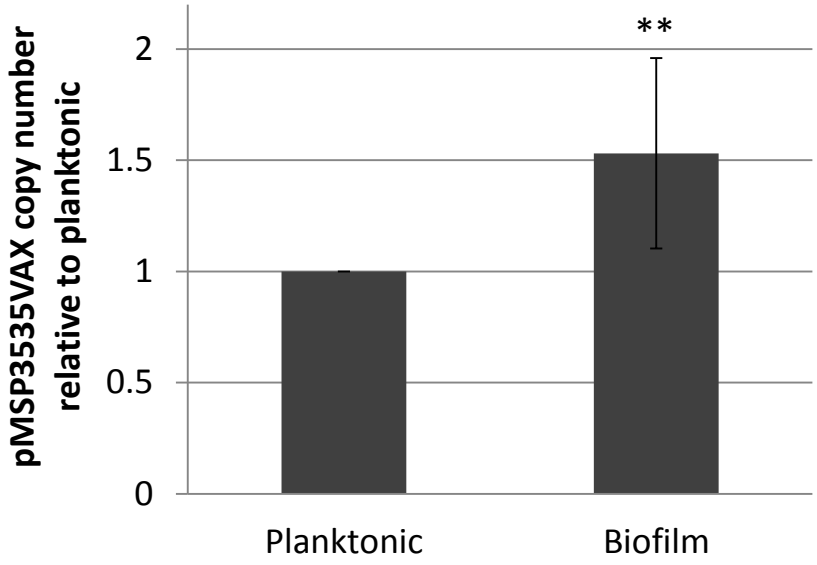

Figure 16. Copy number of pMSP3535VAX is increased as early as 4 hours post-inoculation of the biofilm. Four hour samples of biofilm and planktonic cells were analyzed for pMSP3535VAX plasmid copy number. Planktonic cell copy number is set to 1 and biofilm copy number is shown relative to planktonic copies. **=p value ≤ 0.05 n=3 biological replicates.

In cells containing pCF10, I demonstrated that not only do biofilm cells have a higher average copy number; they also have increased heterogeneity of copy number compared with planktonic cells. To determine whether the same behavior is exhibited by other plasmid replicons, I repeated this experiment with pLC2. pLC2 was chosen because it contains the *prgX-prgQ* operon so cells could be sorted based on induction state, as was done with pCF10. Figure 17A shows a map of the pLC-2 plasmid containing the *prgX-prgQ* operon and a *gfp* gene fused downstream of the Q_L elongation site (see Figure 1 for a more detailed map).

Using this plasmid, I induced biofilm and planktonic cells and then sorted based on GFP expression. As seen earlier, induction of planktonic cells produced a unimodal pattern and induction of biofilm cells resulted in a bimodal distribution (Figure 17B). Following sorting, copy numbers in the populations were examined. As seen in pCF10, the pLC2 plasmid also demonstrated a significant heterogeneity in copy number in biofilm cells that was not present in planktonic cells.

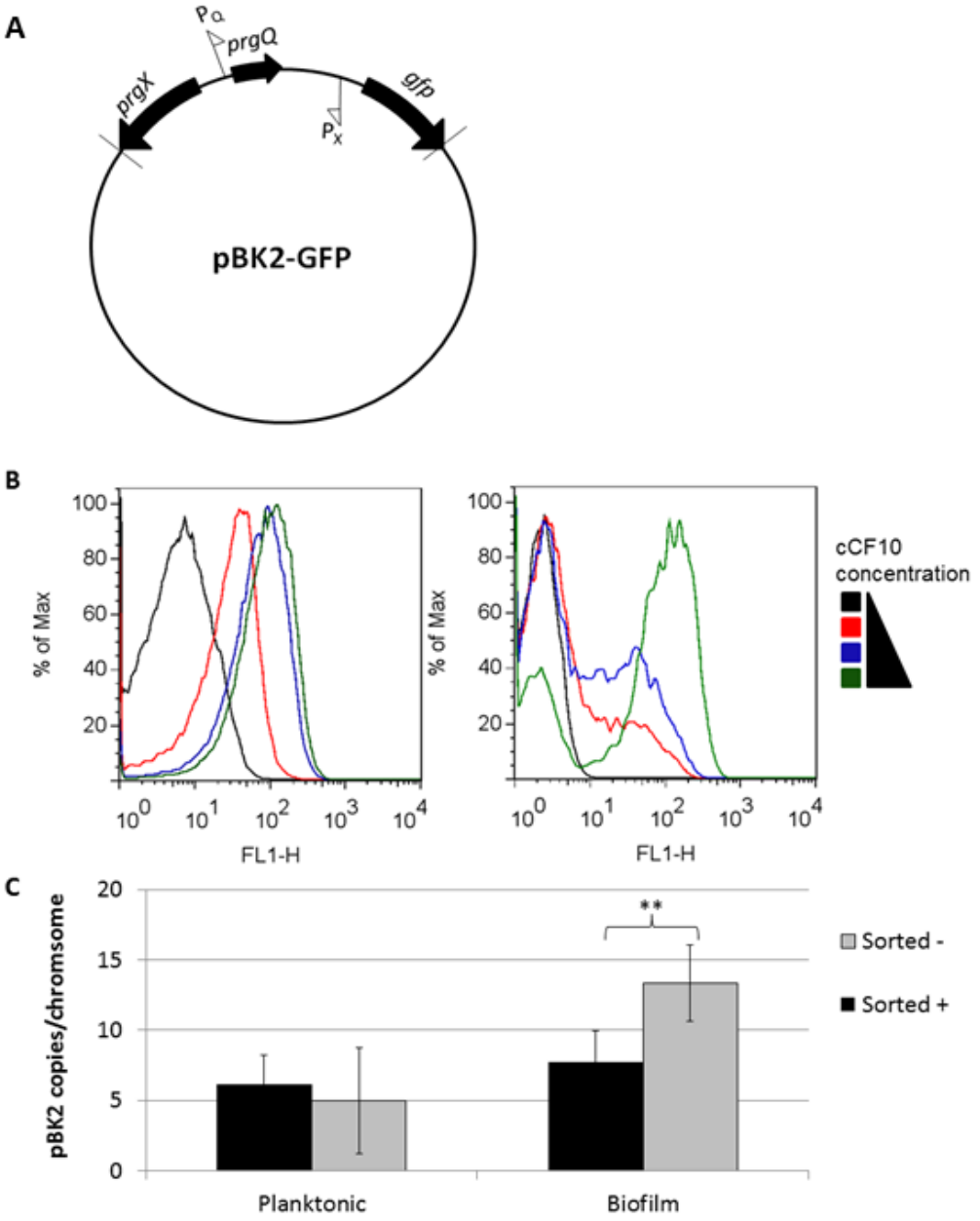

Figure 17. The *prgX*-Q_L portion of the pCF10 plasmid is sufficient to produce bimodal induction of biofilm cells, and sorting of induced cells demonstrates copy number heterogeneity in biofilms that is not present in planktonic populations. A. A plasmid map of the pLC2 plasmid showing the portion of

pCF10 present in the plasmid. The *gfpmut3b* gene was inserted downstream of Q_L RNA. **B.** Following induction with cCF10, only one peak exists in planktonic populations and (left panel) this peak increases in GFP expression. Cells grown in a biofilm (right panel) are induced bimodally following cCF10 induction. **C.** Following sorting of the extreme ends of the peak(s), there is no statistical significance between the edges of induced planktonic populations with all cells containing ~2-6 copies of the pBK2 plasmid per chromosome. In biofilm populations, the two distinct peaks show increased heterogeneity in their copy number from ~5-16 copies per chromosome. **=p value ≤0.05

III. The dual role of iCF10 as inhibitor and quorum sensing molecule

Donor density affects Q_L expression

Quorum sensing via the use of peptide pheromones has been demonstrated in numerous gram-positive bacteria and has been shown to control coordinated activities such as biofilm formation and competence regulation (3, 6). We examined the role of quorum sensing in the conjugative transfer of the pCF10 plasmid of *E. faecalis*. It has been previously suggested that iCF10 is required to prevent self-induction of the donor cells. Because the iCF10 is produced at a basal level in the absence of pheromone induction by cells containing pCF10 and excreted extracellularly. It is possible that iCF10 functions as a quorum signal to sense the population of surrounding donors. We hypothesize that when there is a large population density of donor cells, only a small number would benefit from expending the energy to undergo conjugation when induced. Thus high iCF10 levels would signal high concentration of surrounding donors and prevent induction of the entire population.

Before beginning these studies, we initially tested ratios of iCF10:cCF10 to determine which ratios allowed for complete shutdown of conjugation protein expression (as measured by GFP expression using the pCF10-GFP plasmid). We determined that a 1:1 ratio (in ng/mL) of iCF10:cCF10 did not turn off expression of conjugation genes completely (Figure 18). This result was expected based on previous data indicating that the PrgX protein has a higher binding affinity for cCF10 than iCF10 (25). Using a range of iCF10 and cCF10

concentrations between 0.01-50ng/mL, we observed that a ratio of approximately 10:1 iCF10:cCF10 was needed to establish complete shutdown of the system (Figure 18).

To determine whether cell induction is dependent on the density of donor cells, we examined transcript levels from the P_Q promoter. Cells were diluted 1:10 (high density) or 1:1000 (low density) and induced with various amounts of endogenous cCF10. At the indicated time points, samples were removed, and RNA was collected. RNA was reverse transcribed into cDNA and analyzed via qRT-PCR using primers against a housekeeping gene *gyrB* and Q_L (primers listed in Table 3).

As predicted, cells induced at a high donor density expressed high levels of Q_L but were quickly shut back off (Figure 19A). After 15 minutes, maximal induction levels showed 30-100x more Q_L transcripts than uninduced cells. In as little as 30 minutes, the expression level of Q_L had already decreased significantly returning to basal levels by 1-2 hours (Figure 19A). In low density cell populations, immediate induction of cells was still seen in the first 15 minutes but levels reached 3-5 times that of cells induced at high density. The shutdown observed in high density populations was less pronounced and expression of Q_L was detectable for up to two hours at levels between 50-500xs higher than uninduced cells (Figure 19B).

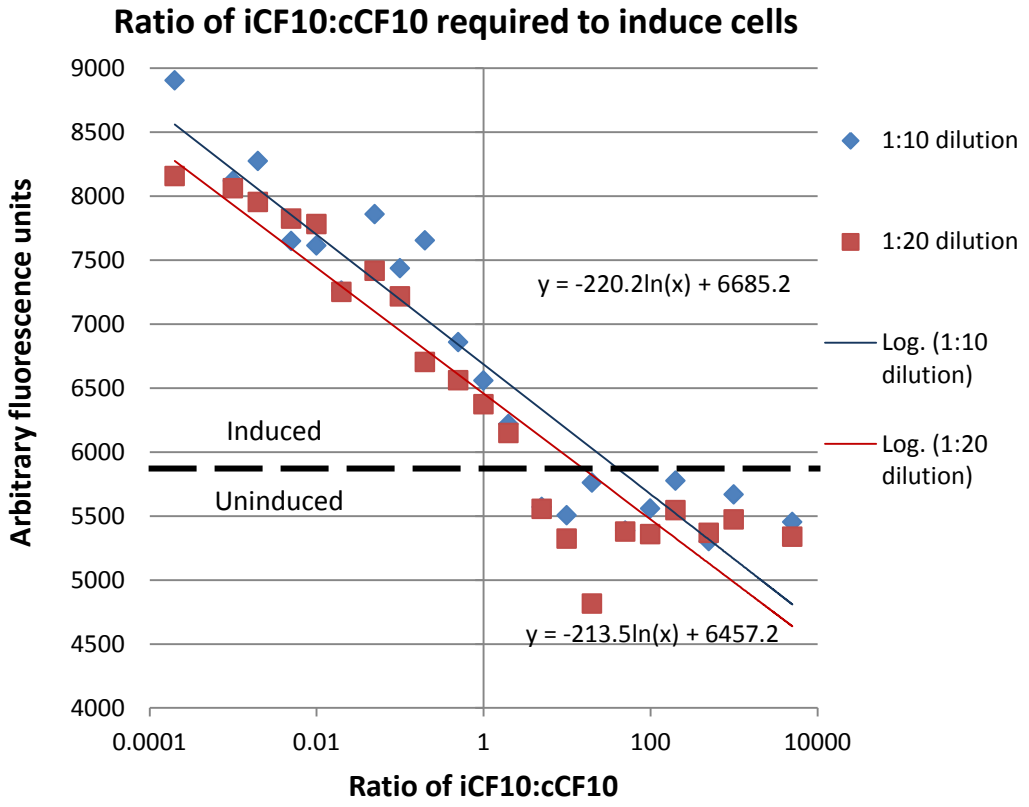

Figure 18. The ratio of cCF10:iCF10 is responsible induction independent of donor density. Cells carrying the pCF10-GFP plasmid were diluted 1:10 or 1:20 and exposed to varying ratios of iCF10:cCF10 and fluorescence levels were measured. At a 1:1 (ng/mL) ratio of iCF10:cCF10, cells were still slightly induced. It takes a ratio of approximately 10:1 iCF10:cCF10 to completely shut off expression of conjugation genes. These results are independent of the initial donor dilution in these ranges.

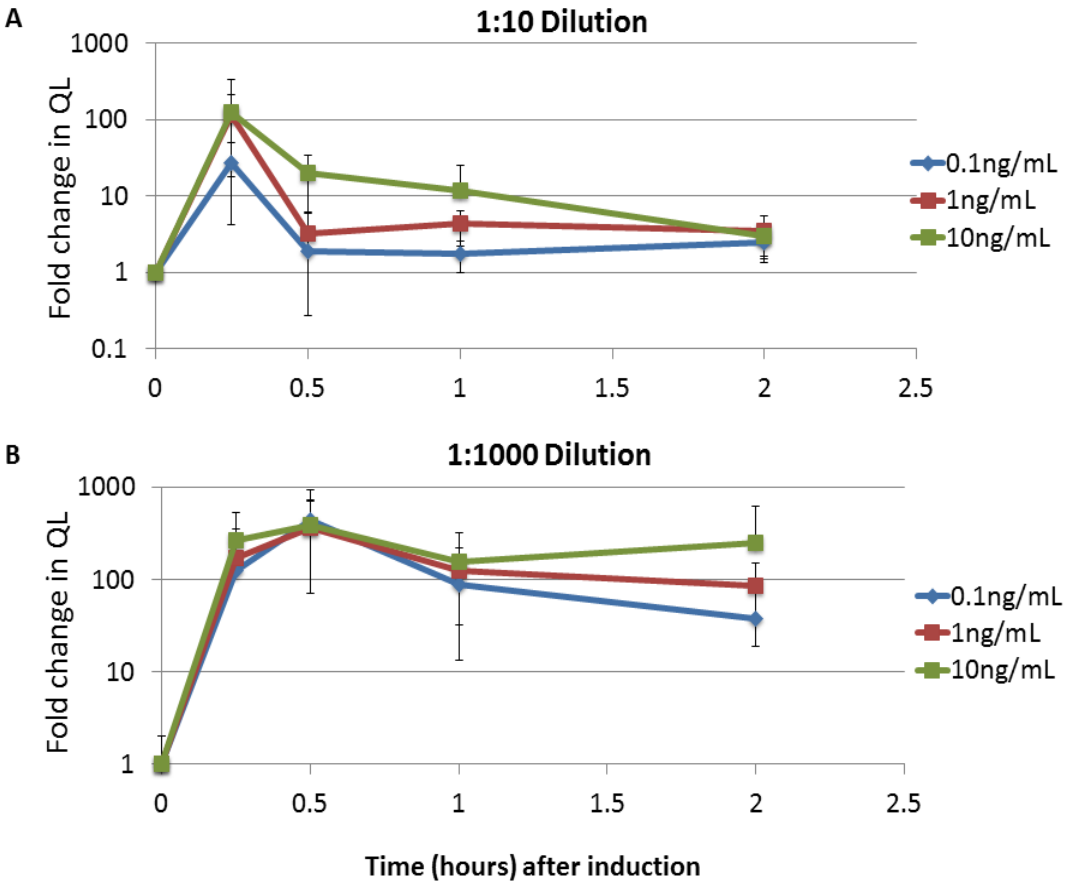

Figure 19. Donor density affects induction and continued expression of Q_L transcripts. A. Cells diluted to high initial donor densities (1:10) were induced to express high levels of Q_L but expression decreased to basal levels by 30-60 minutes. **B.** Cells diluted to low donor densities (1:1000) were induced to higher Q_L expression levels and then remained at high levels for up to two hours post induction. Bars represent the standard deviation for n≥3 biological replicates.

Donor density affects mating frequencies

To determine whether donor density affects conjugation rates, donors were grown overnight and diluted 1:1 or 1:10 before being mixed with recipients (D:R=1:10 v/v). Mating occurred in broth culture for the indicated time, and the samples were plated on antibiotic plates specific for donors, recipients, or transconjugant.

The donor cells that had been diluted 1:1 produced ~1 transconjugant for every 27 donor cells after 3 hours (Figure 20 green line). When the donor cells were diluted 100x lower, 1 transconjugant was made for every ~2.6 donor cells (Figure 20 blue line). The slope of the line between 2-3 hours after mating also demonstrates that mating was still occurring in the dilute donor mating population whereas mating in the high density donor population leveled off (Figure 20).

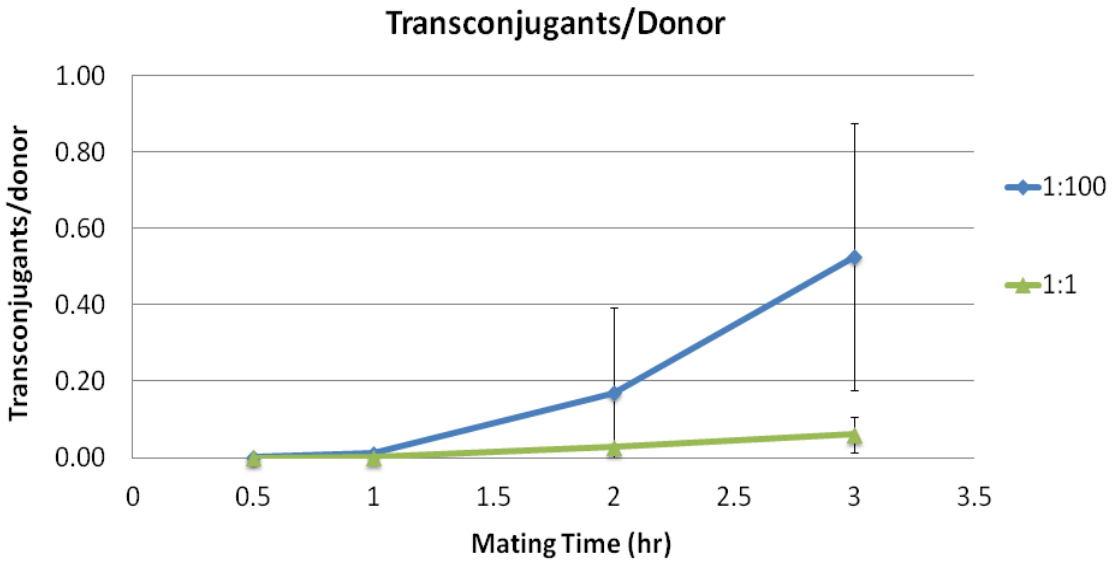

Figure 20. Mating efficiency is affected by donor density. Low density donor populations produce more transconjugants per donor cell than high density donor populations, and conjugation rates continue to increase at later time points.

iCF10 acts to repress induction of Q_L by cCF10

We observed that donor cell density is a determining factor in the expression of conjugation genes. Decreasing the density of donors supports increased expression of conjugation genes and allows this expression to stay relatively constant for a much longer period of time (Figure 19). Cell mating data show a similar phenomenon in which lower donor density allows mating to occur at a higher rate and continue for a longer period of time (Figure 20). These data support a quorum sensing hypothesis in which donor cells are secreting a small molecule capable of signaling donor cell density to surrounding cells to control the induction of conjugation. We hypothesize that donor-produced iCF10 serves this function as well as specifically regulating the expression of Q_L.

Although it has long been hypothesized that iCF10 acts as a direct negative regulator of conjugation gene expression, data proving this theory have been somewhat lacking. To determine the role of iCF10 in quorum sensing and negative regulation, I used a strain of OG1RF deleted for the *eep* gene but containing the pCF10 plasmid (JRC106). Because *eep* plays an integral role in the processing of mature peptides, JRC106 produces no measurable endogenous iCF10 and cCF10. Although small amounts of mature peptide may still be made, these amounts are negligible.

Using JRC106, I examined the role of exogenous peptides in donor density sensing as well as shutdown of Q_L expression. To determine whether iCF10 was in fact responsible for the shutdown of Q_L and, subsequently,

conjugation, we first induced a high density culture of JRC106 with 10 ng/mL exogenous cCF10 for one hour and then added varying concentrations of exogenous iCF10. Q_L RNA levels were quantified using qRT-PCR before induction, following induction, and after addition of iCF10. When JRC106 cells were induced with high levels of cCF10, the level of Q_L transcription increased dramatically (Figure 21A). This result differs from the previous data with the wildtype OG1RF where the Q_L levels had returned to uninduced levels after 60 minutes (Figure 19B). When no iCF10 was added, Q_L levels did not depreciably drop even two hours after the induction. When iCF10 was added to the cultures in levels exceeding cCF10, a statistical decrease was seen in Q_L expression which returned to uninduced levels (Figure 21A). These data strongly suggest that iCF10 is the molecule directly counteracting the inducing effects of cCF10.

To determine whether iCF10 plays a role in donor density sensing, I repeated this experiment using JRC106 at low initial donor densities (1:1000 diluted donors). In one preliminary experiment, the density effects on Q_L expression were eliminated when cells did not produce endogenous iCF10 (Figure 21B). These experiments indicated that not only is iCF10 responsible for the shutdown of Q_L, but endogenous iCF10 also serves as an indicator of donor density. This data will need to be repeated to confirm the findings.

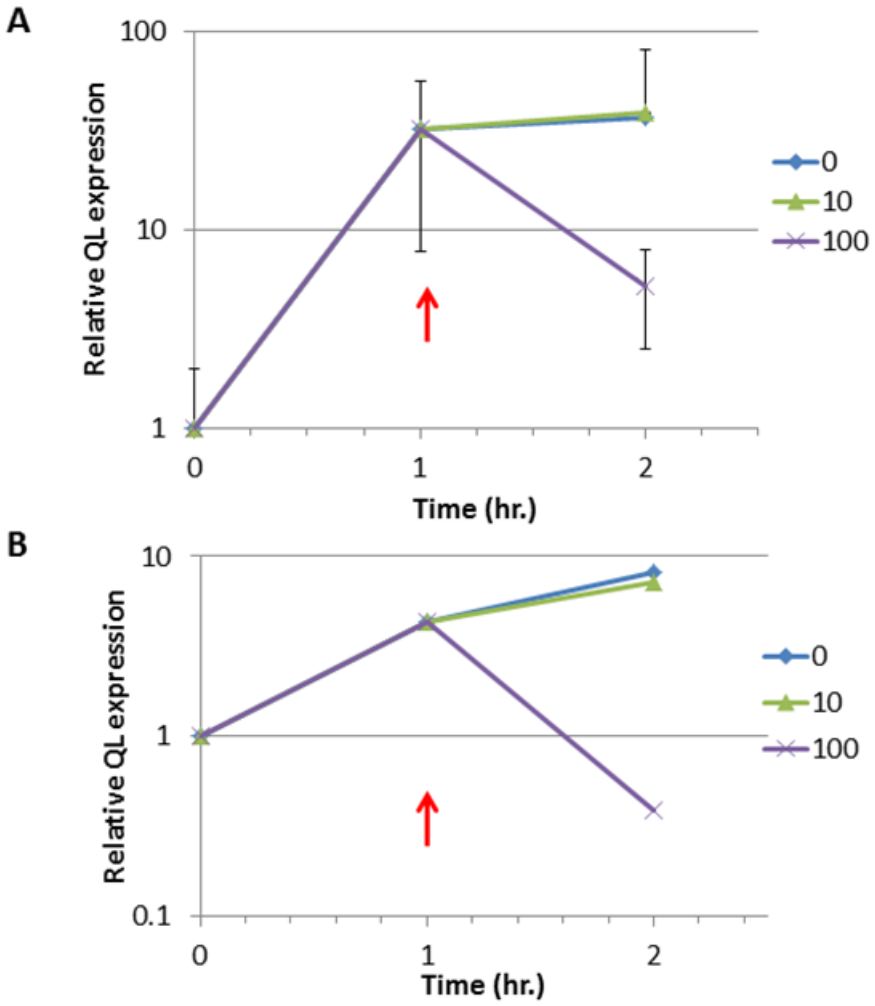

Figure 21. iCF10 is responsible for shutdown of Q_L expression and abolishing endogenous iCF10 abrogates donor density effects on Q_L. Δeep cells (JRC106) containing pCF10 were diluted 1:10 (**A**) or 1:1000 (**B**) and 10ng/mL cCF10 was added at T=0. Cells were grown for 60 minutes with cCF10 before the addition of iCF10 (indicated by red arrow) at varying concentrations (as shown in the graph key).

DISCUSSION

The E. faecalis biofilm transcriptome

Preliminary RNAseq data showed that many genes were up-regulated during the first four hours of biofilm formation. The main categories found to be up-regulated include ABC transporters, and genes involved in metabolism and DNA recombination and repair. I hypothesize that the up-regulation of ABC transporters serves as a mechanism to sample the environment and subsequently alter gene expression based on the changing conditions during early biofilm formation.

Transcriptome analysis also showed that the metabolism of the cells changes dramatically in early biofilms. Pyrimidine synthesis and pyruvate metabolism pathways were both highly up-regulated. A paper published in 2010 by Prüss et al. used a pattern-mining algorithm to determine metabolic enzymes related to biofilm formation. The algorithm predicted that pyruvate catabolism was highly involved in biofilm formation and that acetyl-coenzyme A, a product of pyruvate metabolism, increased biofilm formation in *E. coli* strain K-12 (62). The authors do not posit many hypotheses for why acetyl-CoA might induce increased biofilm formation although they suggest that acetylation of proteins could be important. Proteomics data from *S. aureus* biofilms also demonstrates an important role for pyruvate metabolism in biofilms (53). Interestingly, these two studies were both looking at older biofilms from 8-48 hours old. Pyruvate metabolism, then, is not only involved in the formation of early biofilms, but

continues to occur at high levels throughout at least the first two days of biofilm growth. Although the exact mechanism is not understood, it is apparent that the metabolism of pyruvate, acetyl-CoA and acetate plays an important role in the development of biofilms made by both gram-positive and gram-negative bacteria. This would be an interesting area for future research into biofilm cell metabolism.

My RNAseq data also indicated that genes involved in the DNA repair, recombination, and the SOS response were highly up-regulated in biofilms. Of note, the data indicate that both the activator (RecA) and the repressor (LexA) of the SOS response are up-regulated. LexA has previously been identified to be important in biofilm formation in *P. aeruginosa*, and deletion of *lexA* led to reduced biofilm formation (63). When cells are growing normally, LexA binds to the SOS box in the promoter of SOS genes, including *recA*, and represses their expression. During periods of stress and increased DNA damage, LexA cleaves itself with the help of RecA and relieves repression of the SOS genes. The up-regulation of both *recA* and *lexA* in biofilms is of interest because of their differing roles in the SOS response. If cells are attempting to up-regulate stress responses, why would they concurrently up-regulate the SOS activator and repressor? It is possible that by up-regulating both genes, cells are attempting to up-regulate DNA damage repair but also have a mechanism to keep RecA in check.

Interestingly, a 2008 paper by Boles and Singh identified many of these same genes (eg. *lexA, recA,* and *katA*) as being involved in double-stranded DNA (dsDNA) breaks in biofilm cells when in the presence of oxidative stress (64). The increase in dsDNA breaks lead to an increase in cell diversity in *P. aeruginosa* biofilms which is likely also occurring in *E. faecalis* biofilms (64).

Another question that arises from this data is that while we assume that the biofilm is a more natural environment for bacteria such as *E. faecalis*, why are cells behaving as if the biofilm is a stressful environment? Does something about growth in a biofilm cause DNA breakage that would necessitate increased RecA production? Could this pathway play a role in the increase of extracellular DNA seen in early biofilm matrices? Although the results of the RNAseq data have given us many fascinating answers as to how cells are responding to growth in a biofilm, these data have also provided us with a multitude of new questions for which further research is required.

Currently, studies are being undertaken to enhance our understanding of these data including strand specific analysis and comparison of biofilm and planktonic RNA. It is possible that some of the genes that appear to be up-regulated are in fact antisense transcripts. In this case, genes that would seem to be turned on during biofilm formation may actually be under negative control. Looking at the current RNAseq data and comparing it to promoter trap assays shows that some genes described as lowered in biofilms according to RNAseq had upregulated promoters according to RIVET studies (eg. EF798). Determining

the strand specific RNA transcriptome of biofilm cells will expose many previously unidentified critical biofilm pathways and provide possible gene targets for small molecules to prevent biofilm formation.

RNAseq results demonstrated that a large portion of *E. faecalis* genes are differentially expressed in biofilms when compared to cells grown in liquid culture. These data allowed us to hypothesize that other bacterial systems could be altered by growth in a biofilm. Conjugal gene transfer in enterococci is a significant area of research because of the ability to transfer antibiotic resistance genes. We hypothesized that growth conditions may alter the regulation of conjugative gene induction.

Effects of the environment on conjugation in pCF10

Control of expression of conjugation functions in the pCF10 system is complex and involves competing antagonistic activities of two secreted signaling peptides and multiple intracellular regulatory circuits acting at the level of transcription initiation, as well post-transcriptionally (Figure 1 and (65)). There is experimental evidence demonstrating that the two-peptide signaling system increases versatility such that a response can be activated either by the presence of potential recipient cells in close proximity or by growth in the mammalian bloodstream (66), where expression of the pheromone-inducible *prgB* gene increases virulence (31, 67). However, until recently the relative importance of the multiple (potentially redundant) intracellular mechanisms of regulation of expression of the pCF10 *prgQ* conjugation operon was not clear. Our

collaborators carried out modeling studies and quantitative analysis of transcript levels from the *prgQ* and *prgX* operons in response to cCF10 in planktonic cultures, using genetic constructs to analyze the specific contributions of the individual regulatory mechanisms to the system (68). These studies suggested that the pheromone response system could function as a sensitive bistable genetic switch, and that disruption of any of the individual regulatory circuits of the system abolished switch behavior.

I used a pheromone-inducible GFP reporter construct to allow for expression analysis on a single cell level, and also examined the effects of biofilm growth on the population dynamics of the response. At first glance, the results reported here for planktonic cells appear to be inconsistent with previous studies (68) . However, when the surprising effects of biofilm growth on increasing both the average plasmid copy number and copy number heterogeneity (Figure 12) are considered, the cumulative results are consistent with and validate the predictions of mathematical models put forward by our collaborators (40, 68).

While fluorescent reporter proteins facilitate single cell expression analysis, they do have limitations for our system, including the fact that the fermentative metabolism of enterococci may result in a reduced cytoplasmic environment suboptimal for proper GFP folding. Also, the *gfp* allele used in these studies encodes a very stable protein which may be toxic to cells at very high expression levels. These factors likely reduced the effective signal to noise ratio

in our experiments. I suspect that the apparent lack of bimodal response in planktonic cultures might reflect the limitations of the detection system. It is likely that the low copy number of pCF10 in planktonic cells created a lower threshold for switch behavior to occur and also caused the cells to respond at a lower level blurring the distinction between “on” and “off” as predicted by our mathematical model (Figure 11). In any case, there is a clear difference in the biology of the pheromone response in the two types of cells, with biofilm growth requiring an increased level of signal, but resulting in a more vigorous response to pheromone. This suggested that the average frequency of conjugative plasmid transfer in biofilms could be lower than that of planktonic cells, which was observed experimentally (Table 6).

Plasmid copy number is altered by changing environments

An unexpected result of this study was the effect of biofilm growth on pCF10 copy number (Figure 12). Mathematical modeling suggested that changes in plasmid copy number could account for the observed effects of biofilm growth on the pheromone response (Figure 11 and (40)). While the average copy number of the entire population of biofilm cells was increased, biofilm cells also exhibited a remarkable increase in the heterogeneity of copy number values, which was revealed by analysis of sorted “on” and “off” populations exposed to threshold inducing concentrations of pheromone (Figure 12). As noted above, cells with more copies of pCF10 are more adequately poised to respond to cCF10 pheromone in an appropriate and highly controlled manner than adjacent cells

with lower plasmid copy number (40). By requiring higher pheromone concentrations to turn on conjugation, these cells avoid the expenditure of large amounts of energy involved in producing conjugative machinery. Biofilms are often seen as a type of multicellular community and allowing for conjugation to occur only in a subset of potential donor cells may be beneficial to the community as a whole.

While the bacteria in biofilms are sometimes described as non-growing, or slowly growing, I observed the bimodal pheromone response in cells grown for as little as 4 hours on surfaces, when adherent cell densities were quite low and populations were increasing rapidly. This observation coupled with the apparent unimodal response of planktonic cells grown in a variety of nutrient conditions suggests that aspects of biofilm development not directly related to changes in generation time may affect plasmid copy number and lead to the observed changes in the pheromone response.

This observation was further confirmed by examining the chromosomal content of planktonic and biofilm cells. No difference was observed in the chromosomal content of planktonic and biofilm cells on a per cell basis (Figure 15). This indicates that the difference in copy number observed is not a reflection of chromosomal copy number, but rather a real copy number change.

The mathematical modeling developed by our collaborators suggested that an increase in plasmid copy number would cause an increase in negative regulators such as PrgX and iCF10. This, in turn, could cause more prominent

bistable behavior. Using pLC2, I demonstrated that the P_Q/P_X promoter region and surrounding area is sufficient to see bimodal behavior in cells. As the negative regulators of the system are present in that portion of the plasmid, this result fits with the mathematical modeling prediction.

In terms of pCF10, one can postulate that the increase copy number in biofilms may arise from the need for tighter control of conjugation gene expression. Increased copy number leads to an increase in the overall negative regulators in the cell (i.e. PrgX and iCF10). This allows cells to sense a higher level of cCF10 without turning on. This would be advantageous for *E. faecalis* as it would require potential recipient cells to be in very close proximity to donor cells in order to up-regulate conjugation machinery. As *E. faecalis* cells are non-motile, the need for close cell-cell contact in the biofilm prior to conjugation prevents expenditure of energy if a recipient cell is physically touching the donor cell.

The reduced efficiency of pCF10 transfer in biofilms runs contrary to the popular notion of biofilms being the optimal niche for conjugation (69). The explanation likely relates to the anatomy of enterococci and to differences in the cell attachment mechanisms employed by the conjugative transfer machines of gram positive versus gram negative bacteria. *E. faecalis* has no known mechanisms for active motility in liquids or on solid surfaces. When planktonic cells colonize a surface and initiate biofilm growth, or attach and become part of a pre-existing biofilm, they likely remain in the same location until they either die

or re-enter the planktonic phase by detaching from the biofilm. In the pCF10 system, mating pair formation is mediated by the surface adhesin Asc10 (encoded by *prgB*), which can stably bind the surfaces of cells that randomly collide. There are no extended sex pili that could attach cells that do not come into direct wall-to-wall contact. The evolution of the pheromone response system may have been driven to allow induction of conjugation in biofilms only when donor cells happen to be in extremely close proximity to recipients (perhaps in direct contact), so that the energetically expensive conjugation machinery is only produced when it can be effectively utilized. In planktonic cultures of sufficient population density, random Brownian motion increases the probability of collision between donors and recipients, and induced donors can form stable mating pairs extremely efficiently under these conditions. In this model, the selective pressures for effective spread of the plasmid are balanced by those operating to minimize the metabolic burden of synthesizing the plasmid-encoded proteins. This hypothesis may be tested experimentally by examining conjugation and the pheromone responses of individual donor cells growing in mixed biofilm communities with recipients. We are currently developing the tools such as red fluorescent chromosome reporters to carry out such experiments.

These preliminary data suggested to us that the biofilm environment could be affecting the plasmid makeup of the cell. This is potentially a very significant finding, but I first needed to see if this was a pCF10-specific finding or

a more universal phenomenon. To investigate this further, four plasmids with different backbones and representing both theta and rolling circle replication mechanisms were chosen (Table 8). These four plasmids were grown as biofilms in the CBR and biofilm and plasmid copy numbers were measured using the same protocol as pCF10. Surprisingly, all four plasmids showed significantly higher copy numbers per cell in biofilms as in planktonic cells (Figure 14).

Although this may explain the benefit of increased copy number of pCF10, it does not give any indication as to why other plasmids might undergo similar copy number up-regulation in biofilms. After scouring the literature, one other reference to increased plasmid copy number in biofilms was found. Davies et al. found that, in *P. aeruginosa* biofilms, the plasmid copy number was ~ 1.5 times higher in biofilms than in planktonic cells (70). Only one mention of this was made in the paper, published in 1995, and I could find no further indication that research has been done to explain this phenomenon. If Davies et al. was correct in their observation that copy number is also increase in *P. aeruginosa* biofilms, this phenomenon may be much more widespread than we previously imagined.

This may have many implications in the treatment of biofilm related infections as well as the prevention of antibiotic resistance spread. The physiological basis for the heterogeneity of copy number and pheromone response within the biofilm population is of great interest, and it should be feasible to carry out transcriptome analysis of sorted responsive and non-

responsive biofilm subpopulations, as has been reported for biofilm cells of *Streptococcus mutans* exposed to a competence-inducing peptide pheromone (71).

Donor density and iCF10: Quorum sensing in E. faecalis *conjugation*

In the case of many quorum sensing systems, gene expression is turned on by quorum signals when a certain density is reached. iCF10 signals in *E. faecalis* accumulate at high densities of pCF10-containing donor cells but repress conjugation gene expression rather than activating it. The quorum signal, iCF10, serves not only as an indication of density but also as a direct regulator of conjugation via interaction with PrgX. cCF10, excreted by the plasmid-free recipient cells also acts as a type of quorum sensing molecular, allowing donor cells to sense the presence of recipient cells to initiate conjugation.

Quorum sensing is known to control a wide variety of cellular processes. In our system, data suggest that iCF10 could serve a dual purpose as both a direct negative regulator of conjugation as well as a signal to measure donor density. In this way, *E. faecalis* cells have a unique two-signal system in which cCF10 signals recipient density and iCF10 signals donor density. Both of these signals are required to turn on conjugation and it is their ratio which both signals cell density and activates or represses conjugation (Figure 22).

The data shown here suggest that, in the case of *E. faecalis*, quorum sensing using the iCF10 signal acts to shut down conjugation and thus the spread of antibiotic resistance. Previous studies have suggested that biofilms provide a

niche in which high gene transfer is present (19). The data shown in this thesis refute that assumption for *E. faecalis* biofilms (Table 7). Although the transfer frequencies in biofilm cells are decreased, increased copy number allows them to be uniquely poised to respond very quickly to changes in the cCF10:iCF10 peptide ratio in the environment. We surmise that non-motile cells in a biofilm have adapted a mechanism to precisely monitor the donor and recipient populations in closest proximity to them. This information can lead to increased spread of antibiotic resistance in a population of largely recipient cells. It can also prevent the costly expenditure of individual cell resources on non-productive transfer events or plasmid transfer when the population as a whole is already largely made up of donor cells (Figure 22).

The research presented in this thesis addresses numerous gaps in knowledge about *E. faecalis* biofilms and gene transfer. Data from the RNAseq experiments have provided us with numerous gene targets to investigate biofilm production further in enterococci and related organisms. By linking the biofilm process to conjugation, I have bridged a gap between two seemingly distinct areas of *E. faecalis* biology and pathogenesis. The overlapping systems of quorum sensing, conjugation and plasmid copy number control are now clearer although much is left to be done to fully understand the interplay between these processes.

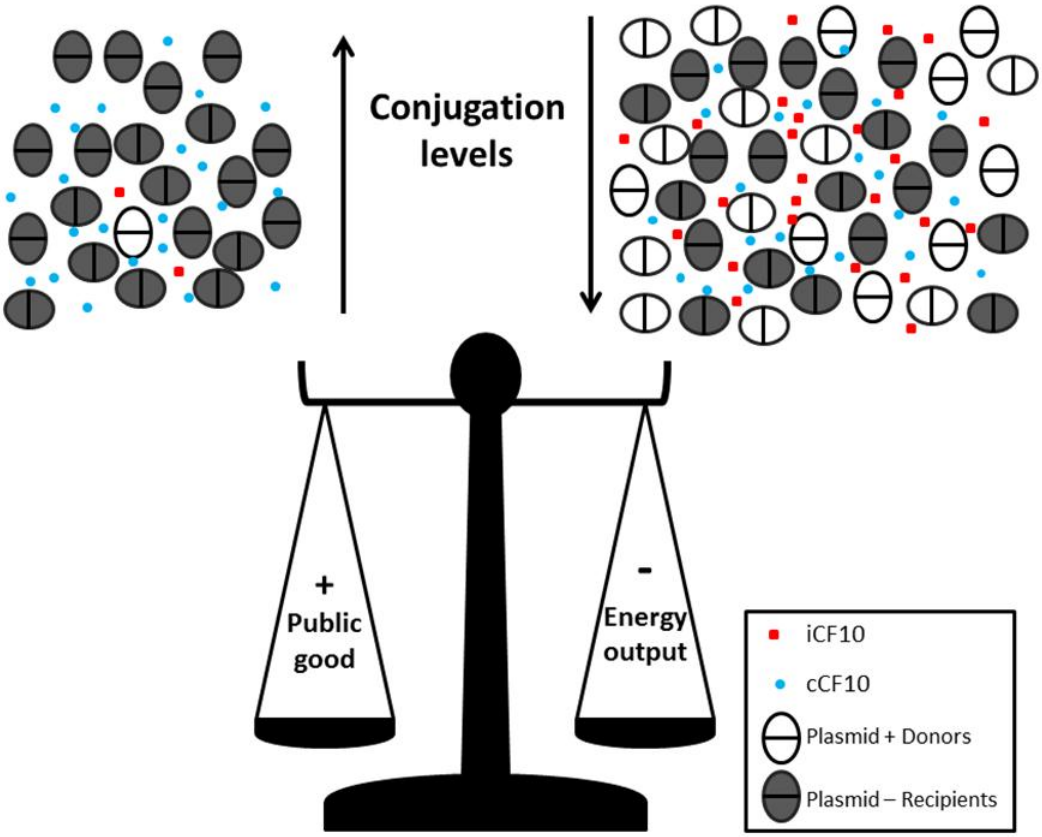

Figure 22. Model of donor density effect on conjugation. In the left panel, the density of recipient cells greatly exceeds donor cells. In this case the iCF10 levels are decreased so conjugation levels are increased. This allows cells to spread the plasmid containing antibiotic resistance to increase the public good. In the left panel, donor density is higher causing iCF10 levels to increase. This shuts down conjugation allowing cells to decrease the energy output of the donor cells in transferring the plasmid. Thus, the quorum sensing system is a delicate balance for the population as a whole.

REFERENCES

1. Gilmore M, editor. The Enterococci: Pathogenesis, Molecular Biology, and Antibiotic Resistance. Washington, D.C.: ASM; 2002.

2. Moellering RJ. Emergence of *Enterococcus* as a significant pathogen. Clin Infect Dis. 1992;14:1173-8.

3. Li T, Lau P, Lee J, Ellen R, Cvitkovitch D. Natural genetic transformation of *Streptococcus mutans* growing in biofilms. Journal of Bacteriology. 2001;183(3):897-908.

4. Boles B, Horswill A. *agr*-Mediated dispersal of *Staphylococcus aureus* biofilms. PLoS Pathogens. 2008;e100052.

5. Ghigo J. Natural conjugative plasmids induce bacterial biofilm development. Nature. 2001;412(6845):442-5.

6. Davies D, Parsek M, Pearson J, Iglewski B, Costerton J, Greenberg E. The invovlement of cell-to-cell signals in the development of a bacterial biofilm. Science. 1998;280:295-7.

7. Duan K, Surette M. Environmental regulation of *Pseudomonas aeruginosa* PAO1 Las andRhl quorum-sensing systems. J Bacteriol. 2007;189(13):4827-36.

8. Lujan S, Guogas L, Ragonese H, Matson S, Redinbo M. Disrupting antibiotic resistance propagation by inhibiting the conjugative DNA relaxase. Proceedings of National Academy of Sciences. 2007;104(30):12282-7.

9. Nguyen K, Piastro K, Gray T, Derbyshire K. Mycobacterial biofilms facilitate horizontal DNA transfer between strains of *Mycobacterium smegmatis*. Journal of Bacteriology. 2010;192(19):5134-42.

10. Nagalakshmi U, Wang Z, Waern K, Shou C, Raha D, Gerstein M, et al. The transcriptional landscape of the yeast genome defined by RNA sequencing. Science. 2008;320(5881):1344-9.

11. Lister R, O'Malley R, Tonti-Filippini J, Gregory B, Berry C, Millary A, et al. Highly integrated single-base resolution maps of the epigenome in *Arabidopsis*. Cell. 2008;133(3):523-36.

12. Sharma CM, Hoffmann S, Darfeuille F, Reignier J, Findeisz S, Sittka A, et al. The primary transcriptome of the major human pathogen Helicobacter pylori. Nature. 2010;464(7286):250-5.

13. Dötsch A, Eckweiler D, Schniederjans M, Zimmermann A, Jensen V, Scharfe M, et al. The *Pseudomonas aeruginosa* Transcriptome in Planktonic Cultures and Static Biofilms Using RNA Sequencing. PLoS ONE. 2012;7(2):e31092. doi: 10.1371/journal.pone.0031092.

14. Ballering K, Kristich C, Grindle S, Oromendia A, Beattie D, Dunny G. Functional genomics of *Enterococcus faecalis*: multiple novel genetic determinants for biofilm formation in the core genome. Journal of Bacteriology. 2009;19:2806-14.

15. Kristich C, Nguyen V, Le T, Barnes A, Grindle S, Dunny G. Development and use of an efficient system for random *mariner* transposon mutagenesis to identify novel genetic determinants of biofilm formation in the core *Enterococcus faecalis* genome. Appl Environ Microbiol. 2008;74(11):3377-86.

16. Nallapareddy S, Singh K, Sillanpaa J, Garsin D, Hook M, Erlandsen S, et al. Endocarditis and biofilm-associated pili of *Enterococcus faecalis*. J Clin Invest. 2006;116(10):2799-807.

17. Hancock L, Perego M. The *Enterococcus faecalis fsr* two-component system controls biofilm development through production of gelatinase. J Bacteriol. 2004;186:5629-39.

18. Cvitkovitch D. Genetic competence and transformation in oral streptococci. Critical Reviews in Oral Biology and Medicine. 2001;12(3):217-43.

19. Molin S, Tolker-Nielsen T. Gene transfer occurs with enhanced efficiency in biofilms and induced enhanced stabilisation of the biofilm structure. Current Opinion in Biotechnology. 2003;14:255-61.

20. Mori M, Sakagami Y, Isogai A, Kitada C, Fujino M, Adsit J, et al. Structre of cCF10nsfer of the Streptococcus faecalis tetracycline resistant plasmid, pCF10. Journal of Biological Chemistry. 1988;263(28):14574-8.

21. Chandler J, Flynn A, Bryan E, Dunny G. Specific control of endogenous cCF10 pheromone by conserved domain of the pCF10-encoded regulatory protein PrgY in Enterococcus faecalis. Journal of Bacteriology. 2005;187(14):13.

22. Nakayama J, Ruhfel R, Dunny G, Isogai A, Suzuki A. The prgQ gene of Enterococcus faecalis tetracycline resistance plasmid pCF10 encodes a peptide inhibitor, iCF10. Journal of Bacteriology. 1994;176(23):4.

23. An F, Sulavik M, Clewell D. Identification and characterization of a determinant (*eep*) on the *Enterococcus faecalis* chromosome that is involved in production of the peptide sex pheromone cAD1. Journal of Bacteriology. 1999;181(19):5915-21.

24. Leonard B, Podbielski A, Hedberg P, Dunny G. *Enterococcus faecalis* pheromone binding protein, PrgZ, recruits a chromosomal oligopeptide permease system to import sex pheromone cCF10 for induction of conjugation. Proc Natl Acad Sci. 1996;93(1):260-4.

25. Kozlowicz B, Bae T, Dunny G. *Enterococcus faecalis* pheromone-responsive protein PrgX: genetic separation of positive autoregulatory functions from those involved in negative regulation of conjugative plasmid transfer. Molecular Microbiology. 2004;54(2):13.

26. Chung J, Dunny G. Transcriptional analysis of a region of *Enterococcus faecalis* plasmid pCF10 involved in positive regulation of conjugative transfer functions. Journal of Bacteriology. 1995;177(8):2118-24.

27. Bae T, Kozlowicz B, Dunny G. Characterization of *cis*-active *prgQ* mutants: evidence for two distinct repression mechanisms by Anti-Q RNA and PrgX protein in pheromone-inducible enterococcal plasmid pCF10. Molecular Microbiology. 2004;51:271-81.

28. Johnson C, Manias D, Haemig H, Shokeen S, Weaver K, Henkin T, et al. Direct evidence for control of the pheromone-inducible *prgQ* operon of *Enterococcus faecalis* plasmid pCF10 by a countertranscript-driven attenuation mechanism. Journal of Bacteriology. 2010;192(6):1634-42.

29. Chatterjee A, Johnson CM, Shu C-C, Kaznessis YN, Ramkrishna D, Dunny GM, et al. Convergent transcription confers a bistability switch in *Enterococcus faecalis* conjugation. Proceedings of the National Academy of Sciences. 2011;108:9721-6.

30. Roux A, Payne S, Gilmore M. Microbial telesensing: probing the environment for friends, foes, and food. Cell Host Microbe. 2009;6(2):115-24.

31. Hirt H, Schlievert P, Dunny G. In vivo induction of virulence and antibiotic resistance transfer in *Enterococcus faecalis* mediated by the sex pheromone-sensing system of pCF10. Infection and Immunity. 2002;70(2):716-23.

32. Hirt H, Manias D, Bryan E, Klein J, Marklund J, Staddon J, et al. Characterization of the Pheromone Response of the *Enterococcus faecalis* Conjugative Plasmid pCF10: Complete Sequence and Comparative Analysis of the Transcriptional and Phenotypic Responses of pCF10-Containing Cells to Pheromone Induction. Journal of Bacteriology. 2005;187(3):1044-54.

33. Kristich C, Chandler J, Dunny G. Development of a host-genotype-independent counterselectable marker and a high-frequency conjugative delivery system and their use in genetic analysis of *Enterococcus faecalis*. Plasmi. 2007;57(2):131-44.

34. Dunny G, Clewell D. Transmissible toxin (hemolysin) plasmid in *Streptococcus faecalis* and its mobilization of a noninfectious drug resistance plasmid. Journal of Bacteriology. 1975;124(2):784-90.

35. Leenhouts K, Buist G, Bolhuis A, tend Berge A, Kiel J, Mierau I, et al. A general system for generating unlabelled gene replacements in bacterial chromosomes. Mol Gen Genet. 1996;353(1-2):217-24.

36. Gold O, Jordan H, van Houte J. The prevalence of enterococci in the human mouth and their pathogenicity in animal models. Archives of Oral Biology. 1975;20:473-7.

37. Dunny G, Brown B, Clewell D. Induced cell aggregation and mating in *Streptococcus faecalis*: evidence for a bacterial sex pheromone. Proceedings of the National Academy of Sciences. 1978;75(7):3479-83.

38. Fixen K, Chandler J, Le T, Kozlowicz B, Manias D, Dunny G. Analysis of amino acid sequence specificity determinants of enterococcal cCF10 sex pheromone in interactions with the pheromone-sensing machinery. Journal of Bacteriology. 2007;189(4):1399-406.

39. Kozlowicz B. The molecular mechanism and peptide signaling response of PrgX used to control pheromone-induced conjugative transfer of pCF10. Minneapolis, MN: University of Minnesota; 2005.

40. Cook L, Chatterjee A, Barnes A, Yarwood J, Hu W-S, Dunny G. Biofilm growth alters regulation of conjugation by a bacterial pheromone. Molecular Microbiology. 2011;81(6):1499-510.

41. Dunny G, Funk C, Adsit J. Direct stimulation and transfer of antibiotic resistance by sex pheromones in *Streptococcus faecalis*. Plasmid. 1981;6(3):270-8.

42. Staddon J, Bryan E, Manias D, Chen Y, Dunny G. Genetic characterization of the conjugative DNA processing system of enterococcal plasmid pCF10. Plasmid. 2006;56(2):102-11. Epub 2006 Jun 13.

43. Bryan E, Bae T, Kleerebezem M, Dunny G. Improved vectors for nisin controlled expression in gram positive bacteria. Plasmid. 2000;44:183-90.

44. Bensing B, Manias D, Dunny G. Pheromone cCF10 and plasmid pCF10-encoded regulatory molecules act post-transcriptionally to activate expression of downstream conjugation functions. Molecular Microbiology. 1997;24(2):285-94.

45. Chung JW, Dunny GM. Cis-acting, orientation-dependent, positive control system activates pheromone-inducible conjugation functions at distances greater than 10 kilobases upstream from its target in *Enterococcus faecalis*. Proc Natl Acad Sci. 1992;89:9020-4.

46. Andersen J, Sternberg C, Poulsen L, Bjorn S, Givskov M, Molin S. New unstable variants of green fluorescent protein for studies of transient gene expression in bacteria. Applied Environmental Microbiology. 1998;64:2240-6.

47. Pfaffl M. A new mathematical model for relative quantification in real-time RT-PCR. Nucleic Acids Res. 2001;29(9):e45.

48. Langmead B, Trapnell C, Pop M, Salzberg S. Ultrafast and memory-efficient alignment of short DNA sequences to the human genome. Genome Biol. 2009;10(3):R25.

49. Natarajan A, Boxrud D, Dunny G, Srienc F. Flow cytometric analysis of growth of two *Streptococcus gordonii* derivatives. Journal of Microbiological Methods. 1999;34(3):223-33.

50. Lazazzera B, Solomon J, Grossman A. An exported peptide functions intracellularly to contribute to cell density singaling in *B. subtilis*. Cell. 1997;89(6):917-25.

51. Beenken K, Dunman P, McAleese F, Macapagal D, Murphy E, Projan S, et al. Global gene expression in *Staphylococcus aureus* biofilms. J Bacteriol. 2004;186(14):4665-84.

52. Naughton S, Parker D, Seemann T, Thomas T, Turnbull L, Rose B, et al. *Pseudomonas aeruginosa* AES-1 exhibits increased virulence gene expression during chronic infection of Cystic Fibrosis lung. PLoS One. 2011;6(9):e24526.

53. Resch A, Leicht S, Saric M, Pasztor L, Jakob A, Gotz F, et al. Comparative proteome analysis of *Staphylococcus aureus* biofilm and planktonic cells and correlation with transcriptome profiling. Proteomics. 2006;6(6):1867-77.

54. Ueda A, Attila C, Witeley M, Wood T. Uracil influences quorum sensing and biofilm formation in P*seudomonas aeruginosa* and fluorouracil is an antagonist. Microbial Biotechnology. 2009;2(1):62-74.

55. Leibig M, Liebeke M, Mader D, Lalk M, Peschel A, Gotz F. Pyruvate formate lyase acts as a formate supplier for metabolic processes during anaerobiosis in *Staphylococcus aureus*. J Bacteriol. 2010;193(952-962).

56. Frank K, Barnes A, Grindle S, Manias D, Schlievert P, Dunny G. Use of recombinase-based *in vivo* expression technology to characterize *Enterococcus faecalis* gene expression during infection identifies *in vivo*-expressed antisense RNAs and implicates the protease Eep in pathogenesis. Infect Immun. 2011;80(2):539-49.

57. Stohl E, Seifert H. *Neisseria gonorrhoeae* DNA recombination and repair enzymes protect against oxidative damage caused by hydrogen peroxide. J Bacteriol. 2006;188(21):7645-51.

58. Konola J, Sargent K, Gow J. Efficient repair of hydrogen peroxide-induced DNA damage by *Escherichia coli* requires SOS induction of RecA and RuvA proteins. Mutat Res. 2000;459:187-94.

59. Arraiano C, Andrade J, Dominiques S, Guinote I, Malecki M, Matos R, et al. The critical role of RNA processing and degradation in the control of gene expression. FEMS Microbiology Reviews. 2010;35(5):883-923.

60. Hayes F, Caplice E, McSweeney A, Fitzgerald G, Daly C. pAMbeta1-associated mobilization of proteinase plasmids from *Lactococcus lactis* subsp. *lactis* UC317 and *L. lactis* subsp. *cremoris* UC205. Appl Environ Microbiol. 1990;56(1):195-201.

61. Trieu-Cuot P, Carlier C, Poyart-Salmeron C, Courvalin P. Shuttle vectors containing a multiple cloning site and a *lacZalpha* gene for conjugale transfer of DNA from *Escherichia coli* to Gram-positive bacteria. Gene. 1991;102(1):99-104.

62. Prub B, Verma K, Samanta P, Sule P, Kumar S, Wu J, et al. Environmental and genetic factors that contribute to *Escherichia coli* K-12 biofilm formation. Arch Microbiol. 2010;192:715-28.

63. Gotoh H, Kasaraneni N, Devineni N, Dallo S, Weitao T. SOS involvement in stress-inducible biofilm formation. Biofouling. 2010;26(5):603-11.

64. Boles B, Singh P. Endogenous oxidative stress produces diversity and adaptability in biofilm communities. Proc Natl Acad Sci. 2008;105(34):12503-8.

65. Dunny G, Johnson C. Regulatory circuits controlling enterococcal conjugation: lessons for functional genomics. Current Opinions in Microbiology. 2011;In press.

66. Chandler J, Hirt H, Dunny G. A paracrine peptide sex pheromone also acts as an autocrine signal to induce plasmid transfer and virulence factor expression in vivo. . Proc Natl Acad Sci. 2005;102(43):15617-22.

67. Chuang O, Schlievert P, Wells C, Manias D, Tripp T, Dunny G. Multiple functional domains of *Enterococcus faecalis* aggregation substance Asc10 contribute to endocarditis virulence. Infection and Immunity. 2009;77(1):539-48.

68. Chatterjee A, Johnson CM, Shu C-C, Kaznessis YN, Ramkrishna D, Dunny GM, et al. Convergent transcription confers a bistability switch in *Enterococcus faecalis* conjugation. Proceedings of the National Academy of Sciences. 2011.

69. Hausner M, Wuertz S. High rates of conjugation in bacterial biofilms as determined by quantitative in situ analysis. Applied and Environmental Microbiology. 1999;65(8):3710-13.

70. Davies D, Geesey G. Regulation of the alginate biosynthesis gene *algC* in *Pseudomonas aeruginosa* during biofilm development in continuous culture. Appl Environ Microbiol. 1995;61(3):860-7.

71. Lemme A, Grobe L, Reck M, Tomasch J, Wagner-Dobler I. Subpopulation specific transcriptome analysis of CSP induced *Streptococcus mutans*. Journal of Bacteriology. 2011;epub.

72. Sotiropoulos V, Kaznessis Y. Synthetic tetracycline-inducible regulatory networks: computer-aided design of dynamic phenotypes. BMC Systems Biology. 2007;1:7.

73. Mehra S, Charaniya S, Takano E, Hu W. A bistable gene switch for antibiotic biosynthesis: the butyrolactone regulon in *Streptomyces coelicolor.* PLoS One. 2008;3(7):e2724.

74. Eguchi Y, Itoh T, J T. Antisense RNA. Annual Reviews in Biochemistry. 1991;60:631-52.

75. Shokeen S, Johnson C, Greenfield T, Manias D, Dunny G, Weaver K. Structural analysis of the Anti-Q-Qs interaction: RNA-mediated regulation of *E. faecalis* plasmid pCF10 conjugation. Plasmid. 2010;64(1):26-35.

76. Bae T, Kozlowicz T, Dunny G. Two targets in pCF10 DNA for PrgX bidning: their role in production of Qa and *prgX* mRNA and in regulation of pheromone-inducible conjugation. Journal of Moleclular Biology. 2002;315(5):995-1007.

APPENDICES

Appendix I. *Unstable GFP variants do not function properly in E. faecalis cells*

Four variants of *gfp* containing peptide sequences on the C-terminal end were tested for fluorescence and half-life in *E. faecalis*. These four variants were first created and tested in *E. coli* and *P. aeruginosa* and shown to have half-lives of approximately 40-60 minutes due to increased degradation of the attached peptide tags and, subsequently, the protein (46). Originally I had hoped to use these variants to study shutdown of the pheromone response.

To determine whether it would be feasible to use these unstable variants as a reporter of gene shutdown, we replaced the *gfpmut3b* gene in pLC2 with each of the four variants. The GFP variants were named after the last three amino acids on the C terminal peptide tags (AAV, LVA, LAA, and ASV). Cells were induced for one hour and then washed before inhibitor iCF10 was added to the culture to downshift GFP expression. In *E. coli*, the LVA and LAA mutants lost approximately 90% of their original fluorescence by 120 minutes post downshift (46). The ASV and AAV variants required longer, approximately 220 minutes for AAV and ASV did not lose more than ~60% fluorescence in 220 minutes (46).

In *E. faecalis,* cells containing the pBK2-LAA fusion, GFP fluorescence did retained wildtype GFP expression levels for 120 minutes. The other three variants, AAV, ASV, and LVA never reached a high enough level of fluorescence to be detectable by fluorometer (Figure 23). Likely the differences between gram-positive and gram-negative bacteria account for the differences in

expression of the fluorescent mutants. Unfortunately, their stability, in the case of LAA, or lack of fluorescence, in the cases of AAV, ASV, and LVA, preclude the use of these GFP variants as gene turnover reporters in our system.

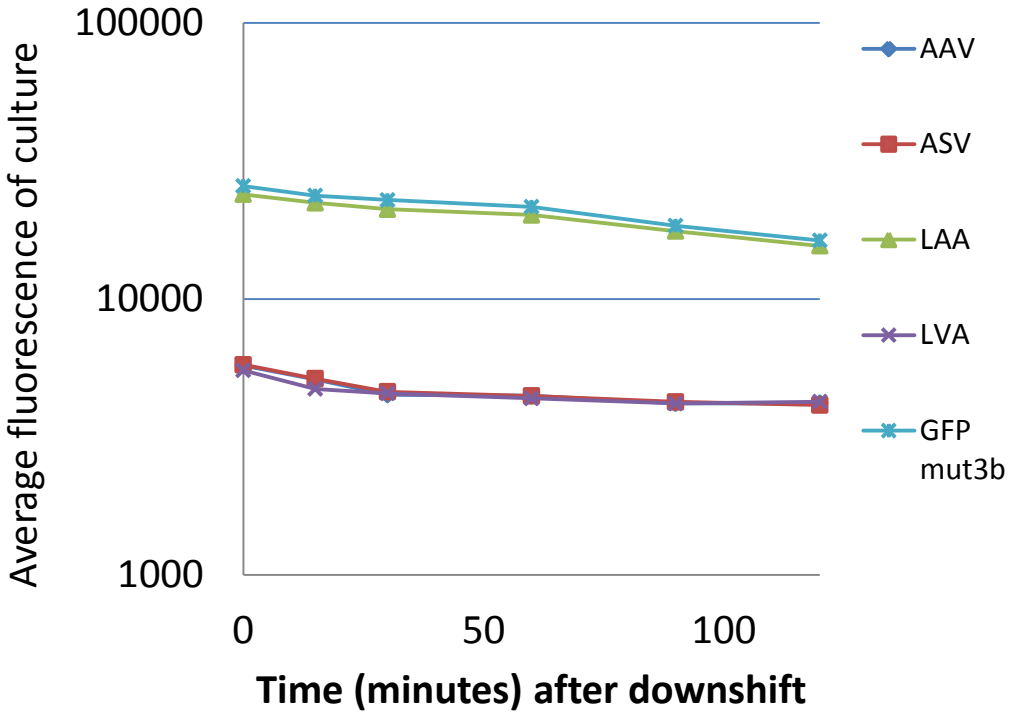

Figure 23. Unstable GFP variants either remain stable or are not expressed properly in *E. faecalis* cells. One unstable GFP variant, LAA, retains high fluorescence and has the same stability as GFPmut3b. Three other GFP variants, AAV, ASV, and LVA, have little to no fluorescence following induction.

Appendix III

Tdtomato does not currently fluoresce optimally in E. faecalis

Although *tdtomato* is constitutively expressed from the chromosome of OG1S, protein expression is patchy with only some of the cells appearing red under the microscope (Figure 24). Cultures were sorted and the 5000 cells with the highest fluorescence were grown up overnight again. When sorted cells were grown overnight, the same patterns of patchy expression of red fluorescence was still seen.

Up to this point, we have been unable to visualize more than ~75% of the population expressing red fluorescence. It is possible that the expression of Tdtomato is costly to the cells and thus they either cause mutations or somehow down-regulate Tdtomato expression. Current experiments examining expression of tdtomato in these cells are ongoing.

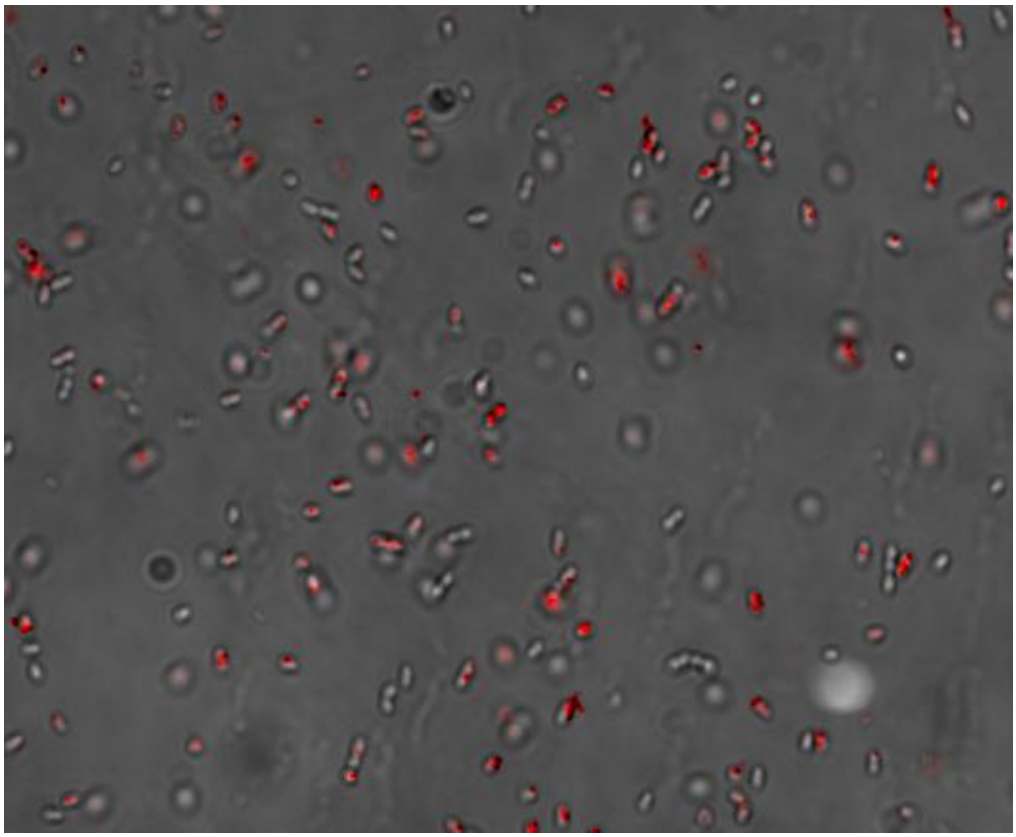

Figure 24. Tdtomato expression in *E. faecalis* cells is inconsistent. Tdtomato is only expressed in a portion of the cells even under control of a constitutive promoter.

Appendix IV

Mathematical modeling parameters

The net rate of production of Q_S and Q_L RNA is given by the first term in Equations 1 and 2 respectively. Expression of PrgB protein is assumed to be proportional to Q_L RNA (Equation 6). The net transcription rate of transcripts Q_S, Q_L and Q_{AR} from P_Q and X and X_{AR} from P_X is denoted by the sum of transcription rate in the uninduced and induced states weighted by concentration of looped [O] to unlooped operator sites ([N]-[O]) respectively as shown in Equations 1-9, where N is the plasmid copy number. The concentration of pCF10 DNA in the looped state ([O]) is given by Equation 10 and has been derived elsewhere (29).

The dynamics of extracellular iCF10 (i), intracellular iCF10 (I) and cCF10 (C) are shown in Equations 7-9. The transport of signaling molecules cCF10 and iCF10 across the cell membrane is modeled as a first order reaction (Equations 8-9). Generation of extracellular iCF10 is modeled as first order with respect to both Q_S and Q_L but not from Q_{AR} as it assumed that truncated RNA does not participate in translation (Equation 7). Degradation and dilution due to cell growth is considered (Equations 1-6 and 8-9). Dilution due to growth is not considered for extracellular iCF10, however, extracellular degradation is considered in Equation 7. The ODEs shown in Equations 1-9 were solved for steady state and dynamic solution for fixed extracellular concentration of cCF10. Steady state response was evaluated for N values from 1 to 25. A characteristic

S-shaped bistable response of PrgB to extracellular cCF10 is predicted (Figure 11B-C).

**All mathematical modeling equations, parameters, and data were derived by our collaborators Drs. Wei-Shou Hu and Anushree Chatterjee.

Table 9. Mathematical modeling equations	
$\frac{d[Q_s]}{dt} = \left(K_{P_{Q_s},U}[O] + K_{P_{Q_s},I}([N]-[O])\right)\left(\frac{K_{P_Q-X_{AR}}\cdot[X_{AR}]}{1+K_{AR}\cdot[X_{AR}]}\right) - (\lambda_{Q_S}+\mu)[Q_s]$	1
$\frac{d[Q_L]}{dt} = \left(K_{P_{Q_L},U}[O] + K_{P_{Q_L},I}([N]-[O])\right)\left(\frac{1}{1+K_{P_Q-X_{AR}}\cdot[X_{AR}]}\right) - (\lambda_{Q_L}+\mu)[Q_L]$	2
$\frac{d[Q_{AR}]}{dt} = [K_{Q_{AR},U}[O] + K_{Q_{AR},I}(N-O)] - K_{AR}[X_{AR}+X]\cdot[Q_{AR}] - (\lambda_{Q_{AR}}+\mu)[Q_{AR}]$	3
$\frac{d[X_{AR}]}{dt} = K_{X_{AR},U}[O] + K_{X_{AR},I}([N]-[O]) - [K_{P_{Q_L},U}O + K_{P_{Q_L},I}(N-O)]\left(\frac{K_{P_Q-X_{AR}}\cdot[X_{AR}]}{1+K_{P_Q-X_{AR}}\cdot[X_{AR}]}\right) - (\lambda_{X_{AR}}+\mu)[X_{AR}]$	4
$\frac{d[X]}{dt} = K_{P_X,U}[O] + K_{P_X,I}([N]-[O]) - K_{AR}[X]\cdot[Q_{AR}] - (\lambda_X+\mu)[X]$	5
$\frac{d[\mathrm{Pr}\,gB]}{dt} = K_{\mathrm{Pr}\,gB}[Q_L] - (\lambda_{\mathrm{Pr}\,gB}+\mu)[\mathrm{Pr}\,gB]$	6
$\frac{d[i]}{dt} = K_i([Q_s]+[Q_L])\cdot V_{conv} - K_{T_i}\cdot[i] - \lambda_i\cdot[i]$	7
$\frac{d[I]}{dt} = K_{T_i}[i] - (\lambda_I+\mu)[I]$	8
$\frac{d[C]}{dt} = K_{T_c}[c] - (\lambda_C+\mu)[C]$	9
$DNA\,loop = [O] = \frac{[N][I]^4}{[I]^4 + K_B[C]^4}$	10

Table 10: List of variables and parameters used in the mathematical model				
Notation	**Description**			
O	DNA of plasmid in loop form			
N	Plasmid copy number,			
Q_S	Q_S mRNA			
Q_L	Q_L mRNA			
X_{AR}	Truncated P_X RNA interacting with Q			
X	X mRNA			
Q_{AR}	Truncated P_Q RNA interacting with X			
i	Extracellular iCF10			
I	Intracellular iCF10			
c	Extracellular cCF10			
C	Intracellular cCF10			
$\mathrm{Pr}gB$	PrgB protein			
Parameter	**Description**	**Value used for bistability**	**Units**	**References**
μ	Specific growth rate of donor cells	2.58×10^{-4}	s^{-1}	(29)
$K_{P_Q,U}$	Transcription rate constant of Q in uninduced state	7.50×10^{-3}	s^{-1}	
$K_{P_Q,I}$	Transcription rate constant of Q in induced state	8.87×10^{-2}	s^{-1}	
$K_{X_{AR},U}$	Transcription rate constant of X_{AR} in uninduced state	1.02×10^{-2}	s^{-1}	
$K_{X_{AR},I}$	Transcription rate constant of X_{AR} in induced state	1.20×10^{-3}	s^{-1}	
$K_{P_X,U}$	Transcription rate constant of X in uninduced state	1.2×10^{-3}	s^{-1}	
$K_{P_X,I}$	Transcription rate constant of X in induced state	1.20×10^{-3}	s^{-1}	
$K_{Q_{AR},U}$	Transcription rate constant of Q_{AR} in uninduced state	1.80×10^{-3}	s^{-1}	
$K_{Q_{AR},I}$	Transcription rate constant of Q_{AR} in induced state	1.53×10^{-3}	s^{-1}	
$K_{\mathrm{Pr}gB}$	Generation rate of PrgB protein	1×10^{-2}	s^{-1}	(72, 73)
K_i	Generation rate of extracellular iCF10	1×10^{-3}	s^{-1}	(29)
V_{conv}	Volume conversion factor	1	-	
K_{T_i}	Transport rate constant of iCF10	1×10^{-3}	s^{-1}	
K_{T_c}	Transport rate constant of cCF10	1×10^{-3}	s^{-1}	
K_{AR}	Rate constant of interaction between X RNA and Q_{AR} RNA	1×10^{-3}	$(nM)^{-1}.\ s$	(74, 75)

$K_{P_Q - X_{AR}}$	Equilibrium constant of Q and X_{AR} interaction	4.43	$(nM)^{-1}$	(74, 75)
K_B	Equilibrium constant of DNA binding reaction	1×10^{8}	-	(22, 29)
λ_{Q_S}	Degradation rate of Q_S mRNA	1×10^{-3}	s^{-1}	(72)
λ_{Q_L}	Degradation rate of Q_L mRNA	1×10^{-1}	s^{-1}	(72)
$\lambda_{X_{AR}}$	Degradation rate of X_{AR} RNA	1.36×10^{-4}	s^{-1}	(76)
$\lambda_{Q_{AR}}$	Degradation rate of Q_{AR} RNA	1×10^{-3}	s^{-1}	(72)
λ_X	Degradation rate of X RNA	1×10^{-4}	s^{-1}	(72)
λ_{PrgB}	Degradation rate of PrgB protein	1×10^{-6}	s^{-1}	(73)
λ_i	Degradation rate of extracellular iCF10	1×10^{-6}	s^{-1}	(73)
λ_I	Degradation rate of intracellular iCF10	1×10^{-6}	s^{-1}	(73)
λ_C	Degradation rate of intracellular cCF10	1×10^{-6}	s^{-1}	(73)